

MODIS DATA STUDY TEAM PRESENTATION

December 22, 1989

AGENDA

1. Status of the MODIS Data Study Team Task
2. GOES IJK/LM Data as MODIS Ancillary/Correlative/Simulation Data
3. Ancillary Requirements for Ocean Color Ancillary Data Sets
4. Science Data Support Team Role and Function (Preliminary)

MODIS DATA SYSTEM STUDY
 APPROVAL
 ACCOMP.

Summary of Deliverables

ORIG. APPUL. 06/24/88
 LAST CHANGE 12/15/89
 STATUS AS OF 01/01/90

| MILESTONES | 89 | | | | | | | | | | | | 90 | | | | | | | | | | | | 91 |
|-----------------------------------|----|---|---|---|---|---|---|---|---|---|---|---|----|---|---|---|---|---|---|---|---|---|---|---|----|
| | M | A | M | J | J | A | S | O | N | D | J | F | M | A | M | J | J | A | S | O | N | D | J | F | |
| 01 Scenarios for Science Team | ▲ | | | | | | | | | | | | | | | | | | | | | | | | |
| 02 Prel TM Sci Prod Summary | ▲ | | | | | | | | | | | | | | | | | | | | | | | | |
| 03 Support MODIS Science Team Mts | | | ▲ | | | | | | | | | | | | | | | | | | | | | | |
| 04 Input Data Attributes Report | | | | ▲ | | | | | | | | | | | | | | | | | | | | | |
| 05 MODIS Data Pkt Recommendation | | | | | ▲ | | | | | | | | | | | | | | | | | | | | |
| 06 Prel Core Prod Algorithm Rep | | | | | | ▲ | | | | | | | | | | | | | | | | | | | |
| 07 Prel TM Core Prod Analysis Rep | | | | | | | ▲ | | | | | | | | | | | | | | | | | | |
| 08 Core Data Proc Scenario Doc | | | | | | | | ▲ | | | | | | | | | | | | | | | | | |
| 09 Post-L'nch Da Proc Sc'rio Doc | | | | | | | | | ▲ | | | | | | | | | | | | | | | | |
| 10 Utility/SUP't Algo Req'ts Doc | | | | | | | | | | ▲ | | | | | | | | | | | | | | | |
| 11 Pres'n to MODIS Sci Team | | | | | | | | | | | ▼ | | | | | | | | | | | | | | |
| 12 MODIS SDST/ICT Req'ts Document | | | | | | | | | | | | ▼ | | | | | | | | | | | | | |
| 13 Proc/Stor&Comm Req'ts Doc | | | | | | | | | | | | | ▼ | | | | | | | | | | | | |
| 14 Core Product Requirements Doc | | | | | | | | | | | | | | ▼ | | | | | | | | | | | |
| 15 MODIS Science Team Mts Support | | | | | | | | | | | | | | | ▼ | | | | | | | | | | |
| 16 Earth-Loc'n Comp'n Req'ts Doc | | | | | | | | | | | | | | | | ▼ | | | | | | | | | |
| 17 Prel L-1 Data Format Document | | | | | | | | | | | | | | | | | ▼ | | | | | | | | |
| 18 Cal'n Algo Implement'n Report | | | | | | | | | | | | | | | | | | ▼ | | | | | | | |
| 19 Prel L-1 Proc Sys Design | | | | | | | | | | | | | | | | | | | ▼ | | | | | | |
| 20 Monthly Reports | ▼ | ▼ | ▼ | ▼ | ▼ | ▼ | ▼ | ▼ | ▼ | ▼ | ▼ | ▼ | ▼ | ▼ | ▼ | ▼ | ▼ | ▼ | ▼ | ▼ | ▼ | ▼ | ▼ | | |

Note:

GOES IJK/LM DATA AS MODIS ANCILLARY/CORRELATIVE/SIMULATION DATA

1. Spacecraft

- Launch of first three-axis stabilized spacecraft in about 18 months
- Two-satellite system provides areal coverage of 1/2 globe
- Imager and sounder operate simultaneously and independently

2. Imager

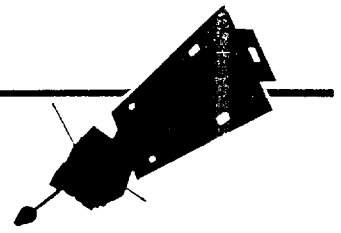
- Five spectral bands: 0.55 to 0.75 μm , 3.8 to 4.0 μm , 6.5 to 7.0 μm , 10.2 to 11.2 μm , and 11.5 to 12.5 μm
- Data rate of 2.6208 Mbps
- High spatial resolution: 1 km visible, 4 km shortwave and longwave thermal infrared, and 8 km moisture thermal infrared
- High sampling rate: 25 minutes for full Earth, 3.1 minutes for 3000 km x 3000 km, 40 seconds for 1000 km x 1000 km
- Pixel location accurate to 2 km at nadir
- Products include surface temperature, moisture imaging, cloud vector winds, cloud height and fraction, day/night imaging of land, water, and clouds, and storm monitoring
- Sensitivities by band (S/N or NE Δ T) are:

| <u>Band</u> | <u>Spec</u> | <u>Plan</u> |
|-------------|-------------|--------------------|
| 1 | 150:1 | 428:1 @100% albedo |
| 2 | 1.4K | 0.09K @ 300K |
| 3 | 1.0K | 0.34K @ 230K |
| 4 | 0.35K | 0.12K @ 300K |
| 5 | 0.35K | 0.15K @ 300K |

3. Sounder

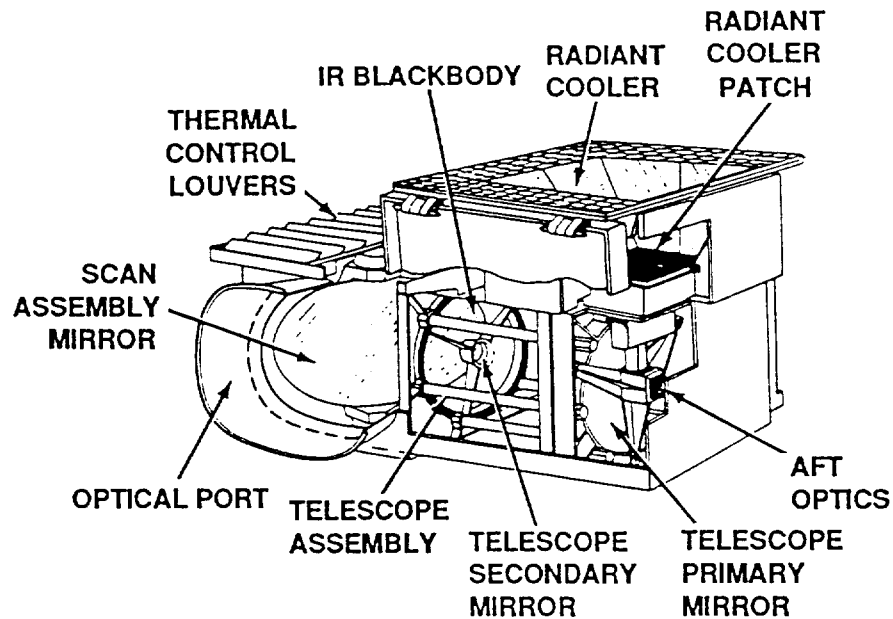
- 19 spectral bands (18 shortwave, midwave, and longwave thermal infrared and one visible)
- Data rate of 40 Kbps
- Spatial resolution of 10 km sample spacing with eight km resolution; 30 to 50 km product horizontal resolution
- Vertical resolution of three km/15 levels
- Sounding rate of three hours for $\pm 50^\circ$ lat/lon of subpoint, 41 minutes for 3000 km x 3000 km, 35 minutes for continental US, and 4.7 minutes for 1000 km x 1000 km.
- Pixel locations accurate to four km.
- Products include vertical temperature and moisture profiles ($\pm 2.5\text{K}$ and 30%, respectively), layer mean temperature and precipitable water ($\pm 2.5\text{K}$ and 20%, respectively), total precipitable water, lifted index, and thermal winds.

GOES



GOES IJK/LM

IMAGING SUBSYSTEM PROVIDES EARTH SCENE IMAGES OF THE WESTERN HEMISPHERE CONTINENTS AND OCEANS



FEATURES

- Earth surface scan from GEO orbit
- Five spectral bands - 0.7 to 12 microns
- High resolution:
 - 1 km visible
 - 4 km shortwave and longwave thermal infrared windows
 - 8 km moisture thermal infrared
- High precision temperature measurement

PRODUCTS

- Day-night imaging of land, water, and clouds
- Surface temperature
- Moisture imaging
- Cloud tracking to obtain winds
- Cloud height and amount
- Storm monitoring



Ford Aerospace

DETAILED IMAGER FEATURES

- Data Rate: 2.6208 Mbps
- Simultaneous imaging from IR & visible channels
- Imaging Rate (frame selectable):

| | |
|-------------------|-------------|
| Full Earth images | 25 minutes |
| 3000 km x 3000 km | 3.1 minutes |
| 1000 km x 1000 km | 40 seconds |
- Combinations of these frames may be pre-programmed and repeated
- Pixel locations accurate to 2 km at nadir
- Independent and simultaneous operation with Sounder
- Mechanically independent and fully stable against other instrument and satellite motions
- Capable of interrupting long duration frames to permit priority (storm watch) observations with repeat-frame option
- Weight, Total: 260 pounds (118 kg)
- Power: 130 watts

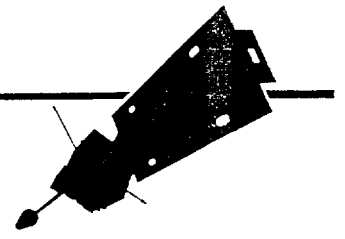
SPECTRAL CHANNELS, DETECTORS, AND PURPOSE

| Channel No. | Wavelength μm | Detector Type | Purpose |
|-------------|--------------------------|---------------|-----------------------------------|
| 1 | 0.55 to 0.75 | Silicon | Cloud and Surface Feature Mapping |
| 2 | 3.80 to 4.00 | In-Sb | Night Mapping |
| 3 | 6.50 to 7.00 | Hg-Cd-Te | Moisture Imaging |
| 4 | 10.20 to 11.20 | Hg-Cd-Te | Thermal Mapping |
| 5 | 11.50 to 12.50 | Hg-Cd-Te | Thermal and Moisture Mapping |

SENSITIVITY

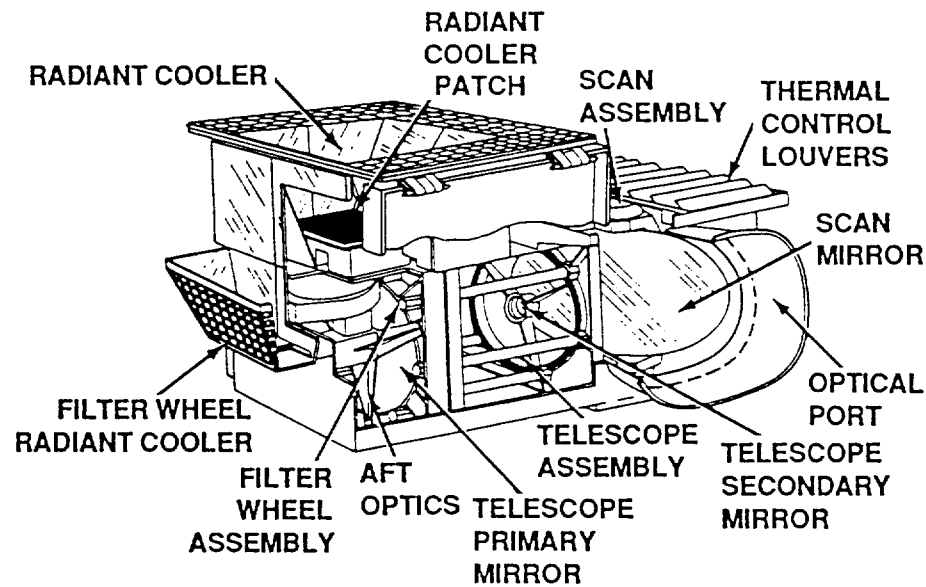
| Channel No. | S/N or NE Δ T | |
|-------------|----------------------|---------------------|
| | Spec | Plan |
| 1 | 150:1 | 428:1 @ 100% Albedo |
| 2 | 1.4K | 0.09K @ 300K |
| 3 | 1.0K | 0.34K @ 230K |
| 4 | 0.35K | 0.12K @ 300K |
| 5 | 0.35K | 0.15K @ 300K |





GOES IJK/LM

**SOUNDING SUBSYSTEM PROVIDES EARTH ATMOSPHERE
VERTICAL TEMPERATURE AND MOISTURE PROFILES**



FEATURES

- Spot surface and atmospheric radiance measurement
- 19 spectral bands - 0.7 to 15 microns
- 10 km sample spacing (nadir) from GEO orbit with 8 km resolution
- Extremely sensitive measurement allows profiles at each spot

PRODUCTS

- Vertical temperature and moisture profiles
- Total precipitable water and precipitable water for three layers
- Cloud height
- Surface radiance and temperature



DETAILED SOUNDER FEATURES

SPECTRAL CHANNELS, DETECTORS, AND PURPOSE

- Data Rate: 40 Kbps

Sounding Rate $\pm 50^\circ$ of subpoint (frame selectable):

50°W - 50°E of subpoint,

50°N to 0°N 3 hours

3000 km x 3000 km 41 minutes

Continental U.S. 35 minutes

1000 km x 1000 km 4.7 minutes

- Scene, each step 280 x 1120 μ radians (10 km x 40 km)
- Combinations of these frames may be pre-programmed and repeated
- Sample locations accurate to 4 km at nadir
- Independent and simultaneous operation with Imager
- Mechanically independent and fully stable against other instrument and spacecraft motions

Capable of interrupting long duration frames to permit priority (storm watch) observations with repeat-frame option

- Weight, Total: 278 pounds (126 kg)
- Power: 105 watts

| Detector | Channel | Wavelength (μ m) | Sensitivity ($NE\Delta N$)* | Purpose |
|-------------|---------|--------------------------|----------------------------------|-------------|
| | 1 | 14.70 | 0.66 | Temperature |
| | 2 | 14.37 | 0.58 | Sounding |
| | 3 | 14.06 | 0.54 | |
| HgCdTe | 4 | 13.64 | 0.45 | |
| (Longwave) | 5 | 13.37 | 0.44 | |
| | 6 | 12.66 | 0.25 | |
| | 7 | 12.02 | 0.16 | Surface |
| | 8 | 11.03 | 0.16 | Temperature |
| | 9 | 9.71 | 0.35 | Total Ozone |
| HgCdTe | 10 | 7.43 | 0.16 | Water Vapor |
| (Midwave) | 11 | 7.02 | 0.12 | Sounding |
| | 12 | 6.51 | 0.15 | |
| | 13 | 4.57 | 0.013 | Temperature |
| | 14 | 4.52 | 0.013 | Sounding |
| InSb | 15 | 4.45 | 0.013 | |
| (Shortwave) | 16 | 4.13 | 0.008 | |
| | 17 | 3.98 | 0.0082 | Surface |
| | 18 | 3.74 | 0.0036 | Temperature |
| Silicon | 19 | 0.696 | 0.10%A | Cloud |
| (Visible) | | | | |

* $MW-M^2-SR^{-1}-CM$



GOES IJK/LM METEOROLOGICAL DATA PRODUCTS

| Data Product | System Accuracy | Horizontal Resolution | Vertical Resolution | Earth Coverage | Observation Frequency | Mission Sensor |
|---------------------------------|--|-------------------------|---------------------|--|--------------------------------|--|
| CLOUD IMAGERY: | Location | | | | | |
| GOES Projection | } ± 4 km | } Vis 1 km IR 4-8 km | } - | } 3/4 - full disk 3000 x 3000 km 1000 x 1000 km | } 15-30 min 5 min 40 sec | } Imager Channels 3 long wave * 1 short wave * 1 visible |
| Mercator Projection | | | | | | |
| Polar Stereo Projection | ± 12 km | Vis 6 km IR 10-18 km | - | Alaska | 15 - 30 min | |
| Composite Images | ± 2 km | Vis 1 km IR 4-8 km | - | Continental US | 15 - 30 min | Imager Vis/11.5 μm IR 11.5/6.7 μm IR |
| CLOUD HEIGHTS: | ± 10 km | 8 km | ± 50 mb | Continental US | 60 min | Imager |
| SOUNDINGS: | vs. Radiosondes | | | | | |
| Vertical Temperature Profile | 2.5° K | 30 - 50 km | 3 km | } Continental US/ adjacent Pacific & Atlantic Oceans | } 60 min- 6 hr | } Sounder 7 long wave * 5 medium wave * 6 short wave * 1 visible |
| Vertical Moisture Profile | ± 30% | 30 - 50 km | 3 km | | | |
| Layer Mean Temperature | 2.5° K | 30 - 50 km | 15 levels | | | |
| Layer Precip - H ₂ O | ± 20% | 30 - 50 km | 15 levels | | | |
| DERIVED IMAGES: | | | | | | |
| Total Precipitable Water | ± 20% | 8 km | - | Continental US | 60 min | Sounder |
| Lifted Index | ± 2 | 8 km | - | Continental US | 60 min | Sounder |
| PRECIPITATION ESTIMATES: | ± 30% of event | 4 km | - | Continental US | 30 min | Imager |
| WINDS: | | | | | | |
| Cloud Drift Winds | Low level 2 - 5 mps High level 5 - 10 mps | 150 - 200 km | ± 50 mb | 50° N - 50° S | 6 hrs | Imager Vis 11.5 μm 6.7 μm |
| Thermal Gradient Winds | 10 mps | 150 - 200 km | 10 levels | 50° N - 50° S | 6 hrs | Sounder |
| Deep Layer Mean Winds | 5 mps | 150 - 200 km | 1 level | 50° N - 50° S | 12 hrs | Imager/Sounder |

* Thermal IR



Ford Aerospace, Space Systems Division, Palo Alto, CA 94303-4697, Phone: 415/852-6989

ACCURACY REQUIREMENTS FOR ANCILLARY DATA SETS
FOR OCEAN COLOR DATA PRODUCTS:
TOTAL OZONE AND ATMOSPHERIC PRESSURE

Remote sensing science begins with a definition of the science requirements, i.e., what scientific questions can be addressed using spaceborne platforms and what geophysical variables can be detected (Figure 1). These requirements drive the instrument design, to ensure that the instrument is capable of detecting, with sufficient accuracy, the radiance signal produced by these geophysical variables. The instrument design defines the acceptable radiance noise levels (the radiometric sensitivity), which impose an absolute limitation on the ability of the instrument to potentially meet the science requirements. Conversion of the radiance detected by the sensor into meaningful geophysical data products then requires a geophysical algorithm, which contains an inherent error. This inherent error has three sources: 1) the instrument radiometric sensitivity, 2) the accuracy of ancillary, external data that may be required for the algorithm, and 3) the inherent accuracy of the algorithm to convert radiance in geophysical variables. This report assesses the accuracy of ancillary data required to meet the radiometric accuracy of the instrument design of MODIS, in relation to ocean color data products. It addresses only one part of this process: the atmospheric correction algorithm.

Three data sets external to the MODIS processing environment have been identified as required in order to produce MODIS ocean color data products. These are 1) total ozone, to determine the absorption of ozone, 2) atmospheric pressure to determine the Rayleigh scattering contribution to the total radiance received by the sensor, and 3) wind speeds to determine the sun glitter and sea foam contributions to the total radiance. These data sets are required for the atmospheric correction of ocean data products, which allows the retrieval of water-leaving radiances. Water-leaving radiances, in turn, are required to obtain all ocean data products based on ocean color, but primary in importance is chlorophyll. Only ozone and atmospheric pressure accuracies are discussed in this report; wind speed accuracies will be discussed elsewhere.

What is required is to know not only what data are needed, but how much, from where the data will be obtained and at what resolution. This report examines the data requirements for ocean color for MODIS, and identifies sources for these data in the MODIS era. Final authority for deciding these accuracy requirements and external data set resolutions rests, of course, with the MODIS Science Team. This report is intended to be a preliminary analysis to estimate requirements of the ocean color atmospheric correction utility/support algorithm and MODIS processing/storage requirements.

The effects of uncompensated variations in total ozone and atmospheric pressure on the retrieval of chlorophyll by the Coastal Zone Color Scanner (CZCS) have been discussed by Gordon et al. (1988a) and Andre and Morel (1989). Both investigators concluded that these variations affected the estimation of chlorophyll, but that the effects were negligible for the CZCS because the errors were less than the minimum detectable radiance (or one digital count) of the CZCS.

MODIS, with 12-bit digitization, has substantially higher radiometric sensitivity than the CZCS, which was 8-bit digitized (Figure 2). This higher radiometric sensitivity imposes stricter requirements on the atmospheric correction algorithm, by making it more sensitive the variability in atmospheric constituents. Furthermore, the additional spectral bands of MODIS in the near-infrared allow a better estimation of aerosols (because water-leaving radiance is near zero here), and consequently, the atmospheric correction algorithm for MODIS will be different from the CZCS. The purpose here is to assess what accuracy of these ancillary data are required to minimize the error in derived products and to maximize MODIS radiometric sensitivity.

Eos (MODIS) Orbital Simulation

To examine the effects of variations in these atmospheric variables on ocean color observations, we tested the sensitivity of the proposed atmospheric correction algorithms (Gordon, 1989) in an extended simulation analysis. In order to realistically simulate these effects for MODIS, we simulated the actual orbit of Eos, important parameters of which are summarized in Table 1.

 Table 1. Orbital parameters of Earth Observing System (Eos) platform used for MODIS orbital simulation.

| | |
|-----------------------|---------|
| Altitude | 705 km |
| Inclination | 98.25° |
| Equator Crossing Time | 1:30 PM |
| Swath Width (Degrees) | |
| --MODIS-T | ± 45° |
| --MODIS-N | ± 55° |

 A series of typical Eos orbits are diagrammatically represented in Figure 3. We chose five locations along the orbit from the Equator northward, denoted by the boxes along the center orbit in Figure 3. These positions correspond to sub-satellite ground points at the Equator, 20°N, 40°N, 50°N, and 60°N. Spacecraft zenith and azimuth angles for these positions were computed using the CZCS Geolocation Algorithm Report (Wilson et al., 1981), modified for the Eos orbital parameters. The sensor scanned across the Earth ground points (pixels) according to MODIS specifications. Solar zenith and azimuth angles were computed from knowledge of the Earth latitude/longitude of the pixel under examination. Computations were performed for the vernal equinox. In the following, MODIS-T was simulated and a tilt of 20° forward was assumed in order to emphasize poor viewing geometry, where errors are accentuated due to increasing atmospheric path length. Solar and spacecraft zenith angles for Earth pixels across the satellite scan are shown in Figure 4 for the five sub-satellite points.

MODIS Radiance Simulation

Realistic ocean water-leaving radiances were computed using the model of Gordon et al. (1988b), given optical properties for five different chlorophyll

concentrations (ranging from 0.5 to 11.0 mg m⁻³) from the model of Sathyendranath and Platt (1988). These models produced expected values of the normalized water-leaving radiance for various chlorophyll concentrations, which is related to the true water-leaving radiance detected by the sensor by

$$L_w = [L_w]_N \cos\theta_o \exp[-(\tau_r/2 + \tau_{oz})/\cos\theta_o] \quad (1)$$

(λ -dependence has been suppressed) where θ_o is the solar zenith angle, τ_r is the Rayleigh optical thickness, and τ_{oz} is the ozone optical thickness. Normalized water-leaving radiances are thus the water-leaving radiance expected for a sun at nadir and with atmosphere removed.

Using these water-leaving radiance values, we constructed a realistic total radiance L_t detected by MODIS by adding Rayleigh scattering radiance L_r and aerosol radiance L_a

$$L_t = L_r + L_a + tL_w \quad (2)$$

where t is the diffuse transmittance from the Earth to the satellite

$$t = \exp[-(\tau_r/2 + \tau_{oz})/\cos\theta] \quad (3)$$

where θ is the satellite zenith angle.

Rayleigh radiance L_r at standard temperature and pressure was computed using a single scattering approximation (Gordon et al., 1983), where τ_r was determined from Hansen and Travis (1974). Mean extraterrestrial irradiance was taken from Neckel and Labs (1984) as averages over the MODIS-T bands, and ozone absorption coefficients were taken from Inn and Tanaka (1953). Aerosol radiance L_a was computed assuming an Angstrom exponent α typical of maritime atmospheres ($\alpha=0.3$; von Hoyningen-Huene and Raabe, 1987), with a radiance at 875 nm of 0.19 mW cm⁻² μm^{-1} sr⁻¹.

Summing L_r , L_a , and tL_w according to Eqn. 2, we constructed a spectral suite of realistic total radiances, from which sensitivity analyses could be performed.

Given L_t , we then used the proposed atmospheric correction of Gordon (1989) to go back and retrieve L_r , L_a , and L_w , and then chlorophyll. In this method, Rayleigh is computed as before, assuming single scattering and standard pressure. Aerosol radiance is computed assuming L_w is zero at 875, 755, and 665 nm, and the Angstrom exponents determined at these wavelengths. The mean of the exponents at 755 and 665 nm was used to estimate the Angstrom exponents at smaller wavelengths, where L_w is not zero. By subtraction

$$tL_w = L_t - L_r - L_a \quad (4)$$

we could obtain the diffusely transmitted water-leaving radiance, and eventually the normalized water-leaving radiance by Eqn. 1. These normalized water-leaving radiances are used to compute chlorophyll by

$$C_1 = 1.15 [L_w(440)]_N/[L_w(560)]_N^{-1.42} \quad (5)$$

for $C \leq 1$ mg m⁻³, and

$$C_2 = 3.64 [L_w(500)]_N/[L_w(560)]_N^{-2.62} \quad (6)$$

for $C > 1 \text{ mg m}^{-3}$ (Gordon, 1988). Eqns. 5 and 6 are called the bio-optical algorithms to distinguish them from the atmospheric correction algorithm, which produce $[L_w]_N$. Errors in chlorophyll according to Eqns. 5 and 6 were also computed in the sensitivity analyses.

It should be noted that Eqns. 5 and 6 do not produce the same chlorophyll concentrations as were originally input to Sathyendranath and Platt's model. This is because Eqns. 5 and 6 were derived empirically, in areas where other optically active substance besides chlorophyll were present. The Sathyendranath and Platt model used here computed optical properties due only to chlorophyll. The new values, computed after atmospheric correction and application of Eqns. 5 and 6 are 0.5, 0.13, 0.9, 3.0, and 8.0 mg m^{-3} .

These data and the methodology to obtain them formed the basis of all analyses.

Total Ozone

Total ozone is required determine the ozone optical thickness and to correct incoming solar irradiance and outgoing water-leaving radiance for absorption by ozone. Ozone optical thickness has a distinct spectral influence, and thus affects most of the ocean core data products.

Figure 5 illustrates the problem in ocean color observations with respect to ozone. Plotted are normalized water-leaving radiances at low ($\approx 0.05 \text{ mg m}^{-3}$), medium ($\approx 1.0 \text{ mg m}^{-3}$), and high ($\approx 8.0 \text{ mg m}^{-3}$) chlorophyll concentrations, along with ozone absorption coefficients ($\times 10$). Since peak ozone absorption is near 560 nm and very low absorption is near 440 nm, errors in estimating the ozone optical thickness will dramatically affect the radiance ratio $[L_w(443)]_N/[L_w(560)]_N$ (also but less so the ratio $[L_w(550)]_N/[L_w(560)]_N$) used to compute remotely sensed chlorophyll.

Errors induced by over- and underestimating total ozone by ± 25 Dobson units (DU) (at an assumed mean of 340 DU) are shown in Figures 6 and 7 for aerosol radiance and normalized water-leaving radiance. These errors were estimated at the sub-satellite position at 50°N (see Figure 3), with the sensor simulating MODIS-T tilted 20° forward, and observing the extreme western edge of the scan. The error in uncompensated ozone is partitioned between aerosol radiance and water-leaving radiance (Figures 6 and 7). Errors in ozone affect the computation of aerosols, because the algorithm uses the radiance at 665 nm, where ozone is absorbing, to estimate aerosol characteristics. Thus an error in ozone "looks" to the algorithm as aerosol. This results in an incorrect Angstrom exponent determination, and produces an error in aerosols and water-leaving radiances that propagates into the short wavelengths, where ozone is only minimally absorbing.

These errors are reflected in the normalized water-leaving radiances (Figure 7), oscillating spectrally between an overestimate and an underestimate. The crossover point in these errors (where the error is zero, at $\approx 500 \text{ nm}$) occurs where the ozone absorption coefficient is the same as at 665 nm (see Figure 5), where the aerosol estimates were generated. At this point, there is no error in $[L_w]_N$ because the aerosol compensates exactly for the error in ozone.

Elsewhere, the aerosol is incorrect, and the water-leaving radiance attempts to compensate. By attempting to compensate, the water-leaving radiance is incorrect both where ozone is more strongly absorbing than at 665 nm, and where it is less, but the error reverses in sign for these two cases. Also plotted in Figure 7 is the minimum detectable radiance for MODIS-N, from the updated specifications report of September, 1989. Noise levels for MODIS-T, as determined from the most recent specifications report (July, 1989) are similar to MODIS-N and are not shown.

Radiance Error

Analysis of the effects of errors in total ozone on the retrieval of $[L_w]_N$ and chlorophyll was based on the five Earth sub-satellite ground positions shown in Figure 3. We assessed the error at five levels of ozone: +5, +10, +15, +20, and +25 DU above mean (340 DU). In all simulations, the error was determined by the difference in radiance (chlorophyll) between computations where the increase in total ozone was accounted for in the atmospheric correction algorithm, and where it was not, i.e., where a mean total ozone was assumed incorrectly. The error thus represents an underestimation of the total ozone. Overestimations were not considered because they merely represent a reverse in the sign of the error. Only errors at the chlorophyll concentration of 0.9 mg m^{-3} are shown because there were insignificant differences in the error in $[L_w]_N$ as a function of concentration.

At the Equator, where a favorable viewing geometry prevailed (spacecraft zenith angle ranging from 65° to 22° ; solar zenith angle ranging from 1° to 40°), the error in $[L_w(440)]_N$ and $[L_w(560)]_N$ is plotted in Figures 8 and 9 (recall from Figure 5 there is no error in $[L_w(500)]_N$ due to ozone; recall also that the maximum error occurred at 560 nm). Also plotted in Figures 8 and 9 is the Noise Equivalent Delta Radiance (NEdL) for MODIS-N at these wavelengths (again MODIS-T NEdL is similar), as an unmarked straight line. This value identifies the noise level for MODIS, and serves as a basis for evaluating the sensitivity of the sensor to ozone variations: if the error due to ozone is less than the NEdL, the high radiometric sensitivity of the sensor is maximized. The NEdL thus serves as a goal for minimizing errors due to ozone and as a threshold for determining the required ozone accuracy to prevent the error from affecting the retrieved water-leaving radiance signal.

From Figures 8 and 9, one may see that an error ± 10 DU is acceptable for $[L_w(440)]_N$ for most of the scan (78%) but exceeds the NEdL for $[L_w(560)]_N$ by about a factor of 2 at the minimum. An error of ± 5 DU is required to meet NEdL requirements for $[L_w(560)]_N$ at the Equator.

At 50°N the solar and spacecraft zenith angles are much less favorable (Figure 4). This location was used as the extreme, since at positions more northward, the solar zenith angle exceeds 60° , where the CZCS experience has shown that ocean color algorithms break down (C.R. McClain, personal communication).

Figures 10 and 11 depict the radiance error $[L_w(440)]_N$ and $[L_w(560)]_N$ at 50°N . Generally, the conclusion remains the same as that derived from the equatorial plots, except that less of the satellite scan falls under the NEdL. However, at these latitudes the MODIS-T scan will overlap with the successive orbit at an untilted scan angle of $\approx 38^\circ$ (as opposed to no overlap at the Equator for either MODIS-T or N), so one need not consider extreme scan angles in the

presented here suggest that full resolution ozone data are required for MODIS, at the highest obtainable accuracy, to meet MODIS radiometric requirements.

The question then arises, can remote sensing data be available for MODIS processing within 24 hours?

If so, then data from other sensors would be ideal for the MODIS ocean color data processing scenario. However, if not, then two other alternatives must be examined. These are: 1) obtaining ozone information from MODIS itself, and 2) processing on MODIS using forecast or previous day ozone estimates.

If ozone scale heights are obtained from the 9.37 μm band on MODIS-N, timeliness requirements for ocean data processing will be met easily, but it is likely that accuracies will be of the order ± 15 DU (Joel Susskind, personal communication). This option must stand as a secondary alternative. A third alternative is to use forecasts or previous day ozone values, perform Level 2 processing, and then update a week or two later using corrected ozone values. This option will produce high quality ocean color data but has a major impact on the processing scenario.

Atmospheric Pressure

Non-standard atmospheric pressure changes the Rayleigh optical thickness and thus affects the atmospheric correction required to obtain MODIS ocean data products. It has been recognized that surface atmospheric pressure observations are required to obtain accurate MODIS atmospheric corrections (Gordon, 1989). This is critical for ocean products because the atmosphere may contribute up to 90% of the total radiance signal received by the satellite.

Andre and Morel (1989) and Gordon et al. (1988a) examined this issue for the CZCS and found that expected variations in atmospheric pressure from standard conditions (1013.25 mb) were about ± 15 mb, considering that very low pressures are usually accompanied by clouds. Given this $\pm 1.5\%$ variation in pressure, the CZCS did not require correction for atmospheric pressure because this error was of the same order as the CZCS pre-launch digital count level (Figure 2). However, they concluded that for ocean color sensors with higher radiometric sensitivity (e.g., MODIS), such a correction was necessary to keep the water-leaving radiance and chlorophyll retrievals within accuracy limits. They did not, however, specify at what accuracy the atmospheric pressure observations were required.

We attempted to assess the atmospheric pressure accuracy required for MODIS through a series of simulations of atmospheric corrections as proposed for MODIS by Gordon (1989). The simulations were similar to those performed for total ozone sensitivity, except that now variations in atmospheric pressure were tested, and total ozone was held fixed at 340 DU. All simulations were performed using single scattering theory for Rayleigh, whereas CZCS and MODIS will likely use the multiple scattering corrections of Gordon et al. (1988a). The result of multiple scattering is to produce more radiance at large atmospheric path lengths than single scattering, but the correction for non-standard pressure is linear for both methods. Thus the increase or decrease in Rayleigh scattering due to non-standard pressure can be equally well represented by single scattering theory as by multiple scattering theory (Andre and Morel, 1989).

accuracy assessment. Considering this, one still arrives at the conclusion that the ozone error must be ≤ 5 DU to meet MODIS NEdL requirements.

Chlorophyll Errors

These radiance errors induce an error in retrieved chlorophyll by changing the ratio of $[L_w(440)]_N/[L_w(560)]_N$ in the bio-optical algorithms (Eqns. 5 and 6). One can see from Figure 5 that underestimating the total ozone will increase the amount of $[L_w(440)]_N$ relative to $[L_w(560)]_N$, thus creating an underestimate in chlorophyll. The reverse situation occurs for an overestimation of ozone.

The errors in chlorophyll using Eqns. 5 and 6 for various underestimations of ozone are depicted in Figure 12 for the sub-satellite position at $50^\circ N$. Gordon (1988) has shown that the bio-optical algorithms contain an inherent error of 18.9%, which is delineated in Figure 12 as a straight line. This requirement is less stringent than that for radiance to meet instrument sensitivity, but still shows that ozone need be known to ± 10 DU in order for chlorophyll errors to fall within the inherent error of the bio-optical algorithm at untilted scan angles up to 38° .

Sensitivity to Aerosol Type

Analysis of these errors due in uncompensated ozone were performed using a typical marine aerosol, characterized by an Angstrom exponent α of 0.3. Angstrom exponents may vary in the marine environment from ≈ 0 to 1 (Gordon, 1988). Thus tests of the effects of uncompensated ozone on the retrieval of water-leaving radiance and chlorophyll were made for Angstrom exponents of 0 and 1. At $\alpha = 0$, normalized water-leaving radiance errors were reduced by 15% compared to that for $\alpha = 0.3$ at 410 nm and 440 nm at an ozone error of +25 DU. This reduction of error was apparently independent of spacecraft position. A negligible difference was noted in $[L_w(560)]_N$. This reduction of error in $[L_w(440)]_N$ resulted in a reduction of error in chlorophyll of $\approx 10\%$.

At $\alpha=1$, errors in $[L_w(410)]_N$ and $[L_w(440)]_N$ increased by a factor of 1.5 over that for $\alpha=0.3$ at +25 DU, which produced 10% more error in the retrieval of chlorophyll. Again negligible differences were noted in $[L_w(560)]_N$. Angstrom exponents near 1 are more typical of continental aerosols than of marine aerosols (von Hoyningen-Huene and Raabe, 1987; Shettle and Fenn, 1979), so the large increase in error due to $\alpha=1$ are probably rare except perhaps near the coast under land breezes.

Sources and Accuracies of Total Ozone Data

Current CZCS processing uses low resolution TOMS (Total Ozone Mapping Spectrometer) data for ozone scale heights, with an accuracy of ± 25 DU (Wayne Esaias, personal communication). This ± 25 DU error level was sufficient for the CZCS, but not for MODIS.

MODIS will require substantially better ozone accuracy in order to keep the radiance error below the NEdL. Current methods for obtaining total ozone from TOMS have accuracies of about ± 10 DU (Joel Susskind, personal communication), but the ± 5 DU requirement for $[L_w(560)]_N$ is expected to be attainable in the MODIS era from HIRS (Joel Susskind, personal communication). The results

Figure 13 shows typical normalized water-leaving radiances and Rayleigh optical thickness at standard pressure. Rayleigh optical thickness has a pronounced spectral effect. Increasing or decreasing the atmospheric pressure changes the Rayleigh optical thickness and hence the Rayleigh radiance. However, if standard pressure is assumed for the atmospheric correction, this change in radiance will be reflected in the total radiance, rather than the Rayleigh radiance, where it belongs.

At a sub-satellite ground point at 50°N, errors in aerosol radiance and normalized water-leaving radiance for uncompensated atmospheric pressure at ± 10 mb are shown in Figure 14 and 15. The extra (or reduced) radiance incurred by pressure ± 10 mb from standard was partially divided between aerosol radiance and water-leaving radiance, as for ozone errors. Note the Rayleigh-like shape of the errors in Figures 14 and 15. The error in $[L_w(440)]_N$ and $[L_w(560)]_N$ would represent a chlorophyll concentration of $\approx 0.07 \text{ mg m}^{-3}$, so that at chlorophyll concentrations above this amount, the error in underestimating atmospheric pressure produced an underestimate of chlorophyll, and at levels below this value, produced an overestimate. Interestingly, at a "real" chlorophyll concentration of 0.07 mg m^{-3} , there is no error in retrieved chlorophyll, regardless the error in atmospheric pressure.

Radiance Error

Errors in retrieved normalized water-leaving radiance were assessed at underestimations of the atmospheric pressure by 0.5 mb, 1 mb, 5 mb, and 10mb. As a consequence, "extra" radiance in the total radiance signal was not removed by the Rayleigh approximations, and turned up in the aerosols and $[L_w]_N$. Errors were assessed at 410 nm because, as can be seen in Figure 15, they are greatest here, and at 440 nm because of its relevance to the bio-optical algorithms. Errors at $[L_w(560)]_N$ are not shown because they do not change the basic result. Radiance errors were independent of chlorophyll concentration, so only those at 0.9 mg m^{-3} are shown.

Atmospheric pressure is required to be known to ± 0.5 mb to meet the MODIS NEdL for $[L_w(410)]_N$ for a significant portion of the scan when the satellite ground point is 50°N (Figure 16). However, an accuracy of ± 1 mb is within 2NEdL over most of the scan and meets the NEdL requirements for $[L_w(440)]_N$ over most of the scan (Figure 17).

Chlorophyll Error

Again because of the inherent error in the bio-optical algorithms, the atmospheric pressure accuracy requirement is loosened for chlorophyll. In fact, up to about a 35° untilted scan angle (which very nearly overlaps with a 35° scan from the successive orbit at this latitude), pressure accuracy of ± 5 mb is sufficient (Figure 17). (Only the error at 0.9 mg m^{-3} chlorophyll is shown because generally this level represented the maximum error). If the pressure is known to ± 1 mb or less, all of the scan falls under the algorithm uncertainty, even at 50°N.

Sensitivity to Aerosol Type

Changing the aerosol Angstrom exponent α from 0.3 to 0 resulted in only a minor change in the results of atmospheric pressure accuracy. Tests were

performed for an underestimation of pressure by 10 mb. Error in $[L_w(410)]_N$ and $[L_w(440)]_N$ increased by only 5-6% at $\alpha=0$ over that for $\alpha=0.3$ for all sub-satellite locations. Changes in chlorophyll error were negligible. When α was set to 1, the error in $[L_w(410)]_N$ and $[L_w(440)]_N$ decreased by 15-18%, and chlorophyll error dropped by 2-3% over all locations. This decrease resulted from the fact that at $\alpha=1$, the error in aerosol radiance more closely resembled the Rayleigh error induced by uncompensated pressure. Generally, the aerosol type had minor effect on the assessment of pressure accuracy requirements.

Sources and Accuracy of Atmospheric Pressure Data

Unfortunately, atmospheric pressure accuracy of ± 0.5 mb is probably an unrealistic expectation for the MODIS era. Wayman Baker of NOAA, however, suggested that an accuracy of ± 1 mb in National Meteorological Center) NMC synoptic analyses is probably realistic for the MODIS time frame for the northern hemisphere. At ± 1 mb, the maximum error in chlorophyll is $< 10\%$ even at $50^\circ N$, and $< 5\%$ elsewhere. Also, the absolute error in $[L_w]_N$ is within ± 2 times the minimum detectable radiance.

Thus, given an accuracy of ± 1 mb, the residual error in $[L_w]_N$ and chlorophyll may be considered acceptable. It also appears that ± 1 mb is attainable, at least for the northern hemisphere. For the southern hemisphere, errors may be as large as several mb (Wayman Baker, personal communication), and thus the accuracy of radiance and chlorophyll retrievals will be less here. But the accuracy goal of ± 1 mb in atmospheric pressure appears at this time to be a reasonable and achievable standard.

If one assumes that pressure changes are of the order 1 mb per 100 km, then the above analysis suggests a requirement of 50 km NMC synoptic atmospheric pressure analyses (incorporating Nyquist frequency considerations) for the MODIS ocean processing scenario for atmospheric corrections. Wayne Esaias at GSFC pointed out that AIRS or MODIS oxygen soundings may provide an alternate source of atmospheric pressure data. However, such a procedure is not refined at this time and requires further research.

Discussion

These analyses were based on the premise that the high radiometric sensitivity of MODIS be maximized. Under such premise, errors in normalized water-leaving radiance induced by non-standard total ozone or atmospheric pressure must be kept below the MODIS noise level (NE_{DL}) in order to prevent their having an effect on ocean color. This is an extremely rigorous standard, and the analyses showed that total ozone and atmospheric pressure must be known to the limits of their present accuracies (± 5 DU for ozone; ± 0.5 mb for pressure) in order to meet this standard for substantial portions of the satellite scan and Earth coverage.

However, Gordon (1988) showed that the inherent error of relating normalized water-leaving radiances to chlorophyll through the bio-optical algorithms (Eqns. 5 and 6) was 18.9% for Eqn. 5 and 27.3% for Eqn. 6. Considering this, radiance errors in $[L_w(440)]_N$, $[L_w(500)]_N$, and $[L_w(560)]_N$ must be 0.045, 0.037, and $0.024 \text{ mW cm}^{-2} \mu\text{m}^{-1} \text{ sr}^{-1}$, respectively. This is approximately equivalent to one CZCS digital count and imposes a much less strict requirement on acceptable radiance errors, and hence ozone and pressure errors. At this

standard, ozone must be known to ± 10 DU and pressure to ± 5 mb to maximize Earth coverage and the satellite scan.

The inherent error in the bio-optical algorithm, however, assumes no improvement. One of the purposes of the large spectral coverage of MODIS is to infer the dependence of the radiances used in the bio-optical algorithms on in-water optical constituents besides chlorophyll (e.g., gelbstoff, detritus, coccoliths, suspended sediments). This will require use of other spectral bands to quantify these constituents, and their effect on $[L_w]_N$ at 440, 500, and 560 nm may then be removed, allowing improvement of the algorithm. This procedure requires that $[L_w]_N$ be known to high accuracy, and suggests that the goal of maximizing MODIS sensitivity set requirements on the ancillary atmospheric data in the atmospheric correction.

Finally, all simulations were performed for a solar declination point at the Equator. This simulates a sort of "average" solar position, but useable Earth coverage by MODIS will change depending on time of year, and thus affect the accuracies required for ozone and pressure. For example, in the northern hemisphere winter, solar zenith angles less than 60° will occur up to $\approx 70^\circ$ N latitude. At this latitude orbital overlap is much greater than at 50° N, and scan angles out to only $\approx 28^\circ$ are required to produce full Earth coverage. This reduces the error due to ozone and pressure and reduces the ancillary data requirements. Earth coverage in the southern hemisphere at this time, however, is much reduced and requirements will be stricter. The vernal equinox is a good standard by which to assess accuracy requirements under most operating conditions.

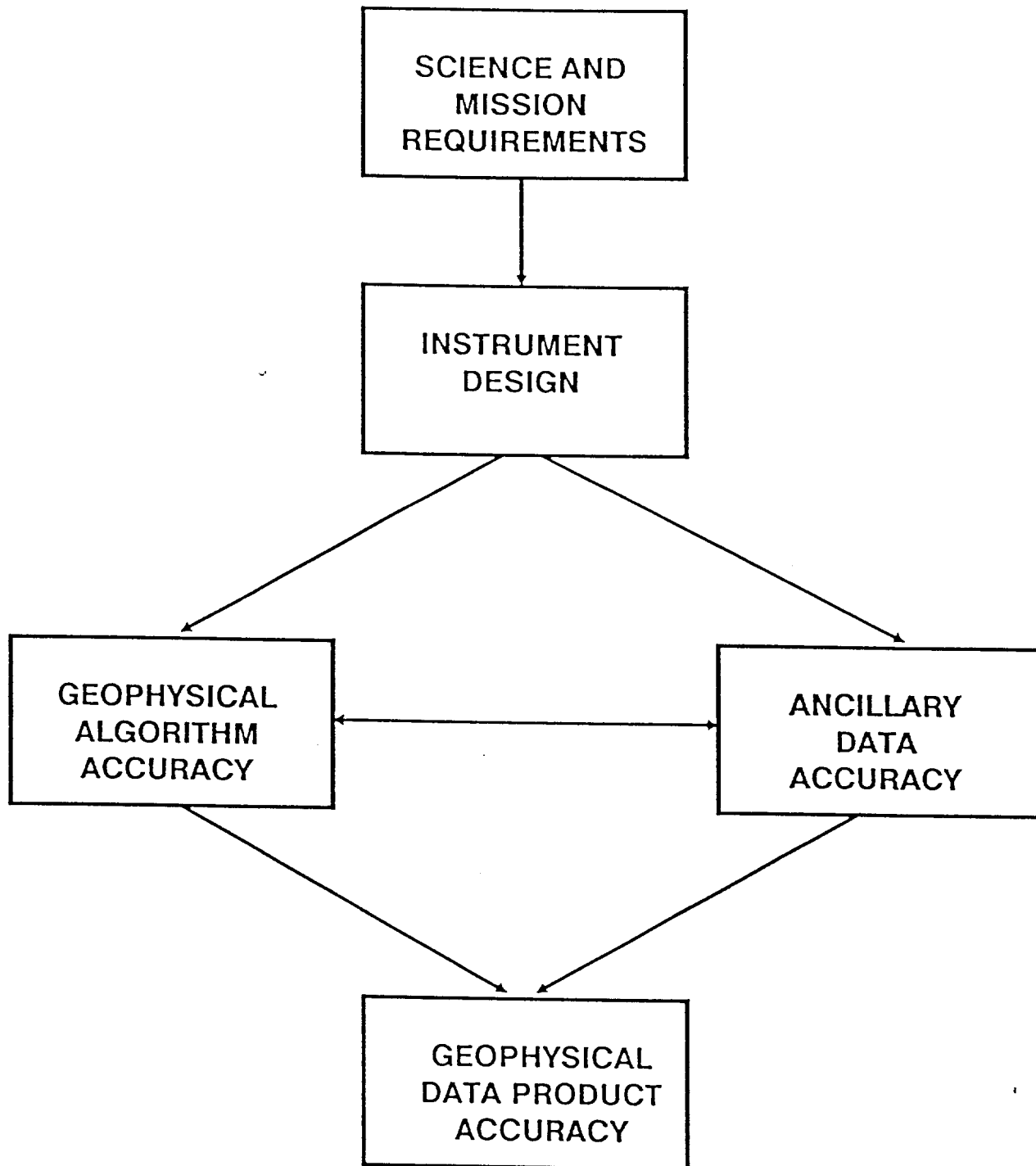


Figure 1. Diagram of the relationships between science requirements, instrument design, geophysical algorithms and ancillary data accuracies required in a remote sensing mission.

Noise Levels

MODIS-N,T and CZCS

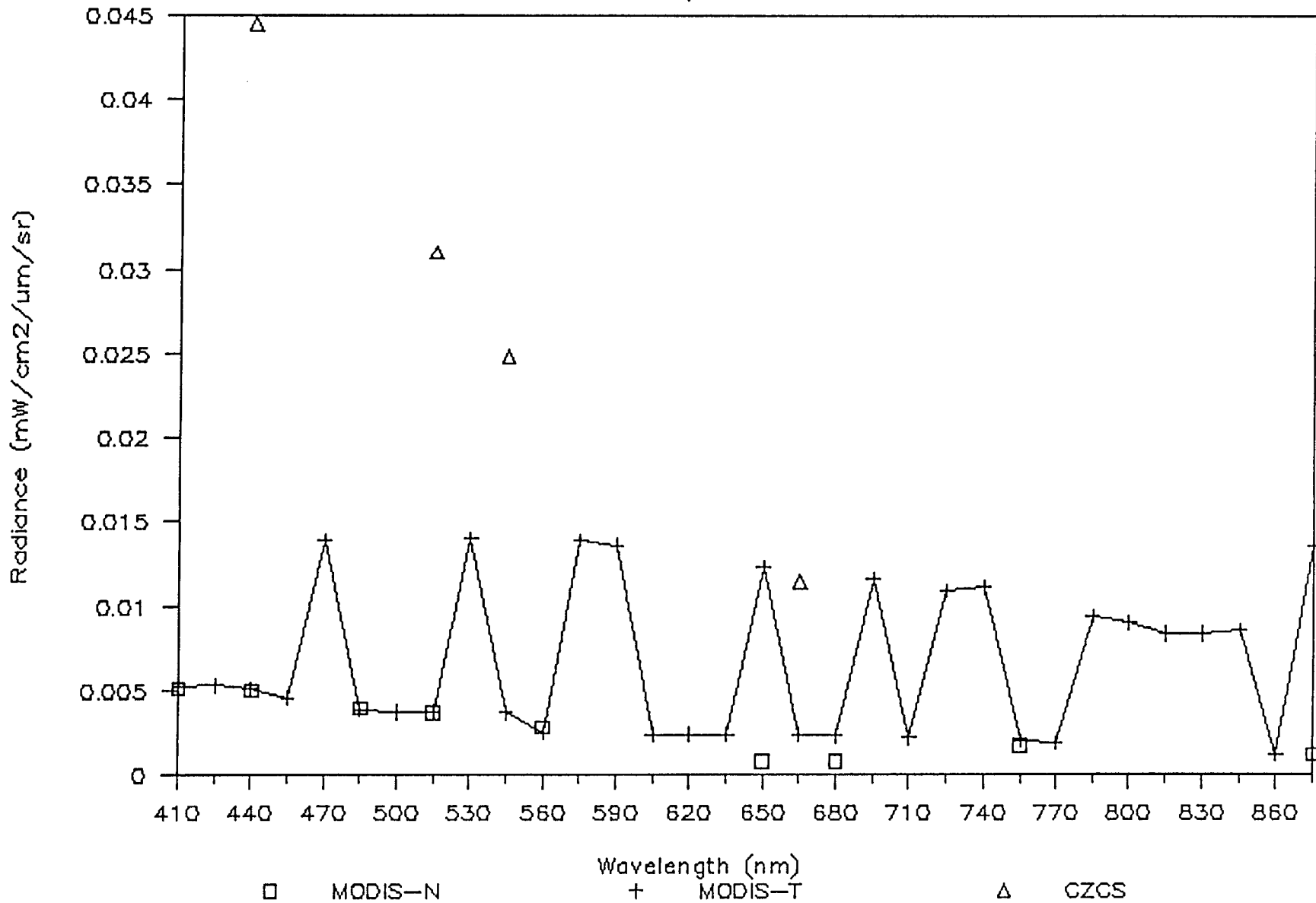


Figure 2. Noise equivalent delta radiance levels for MODIS-T and MODIS-N, and the radiance level of one digital count for the CZCS.

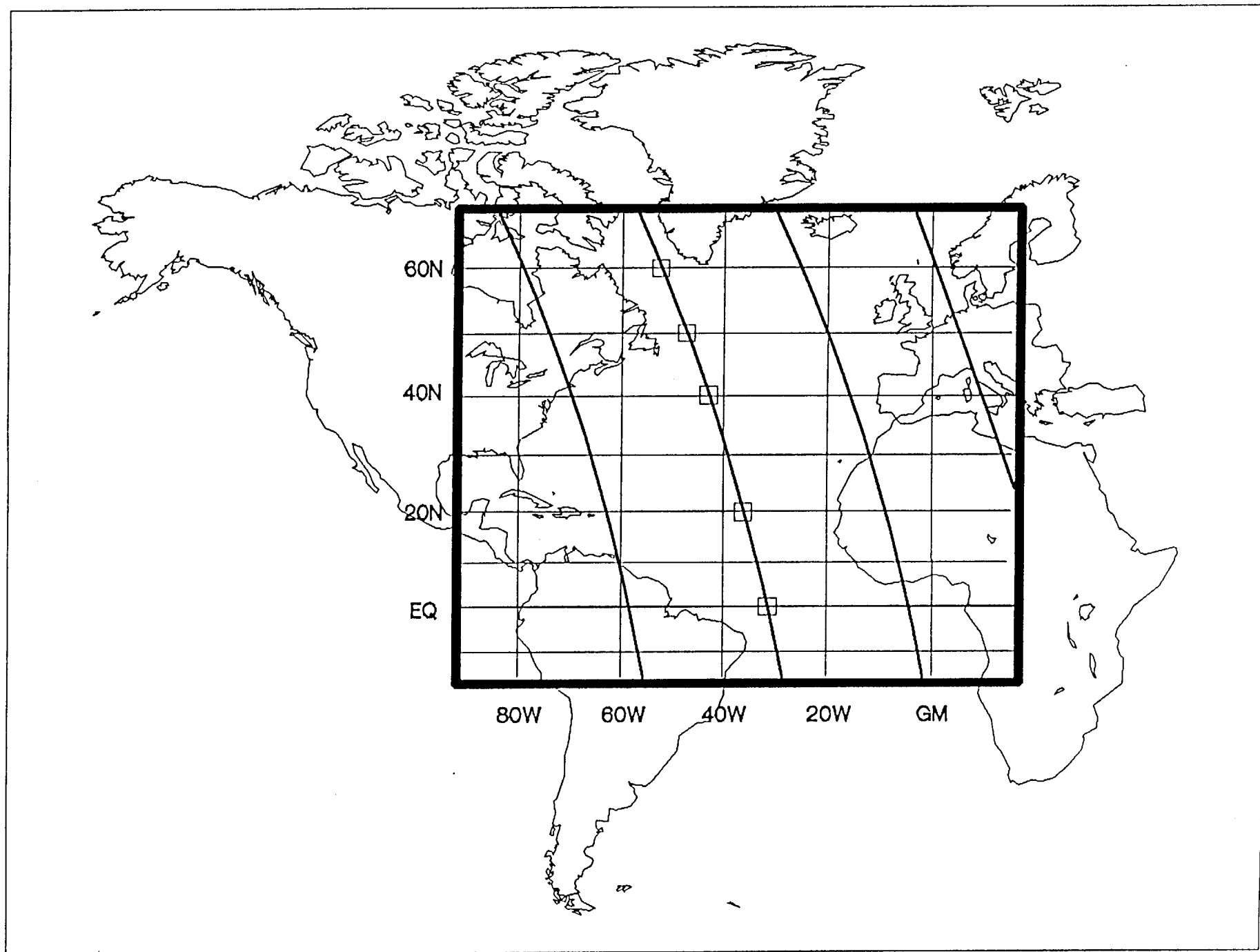


Figure 3. Representation of Eos orbital tracks used in the simulation analyses. Boxes indicate Earth locations where of the sub-satellite ground point where assessments of ozone and atmospheric pressure were made.

Normalized Water-Leaving Radiance

Ozone Absorption Coeff. ($\times 10$)

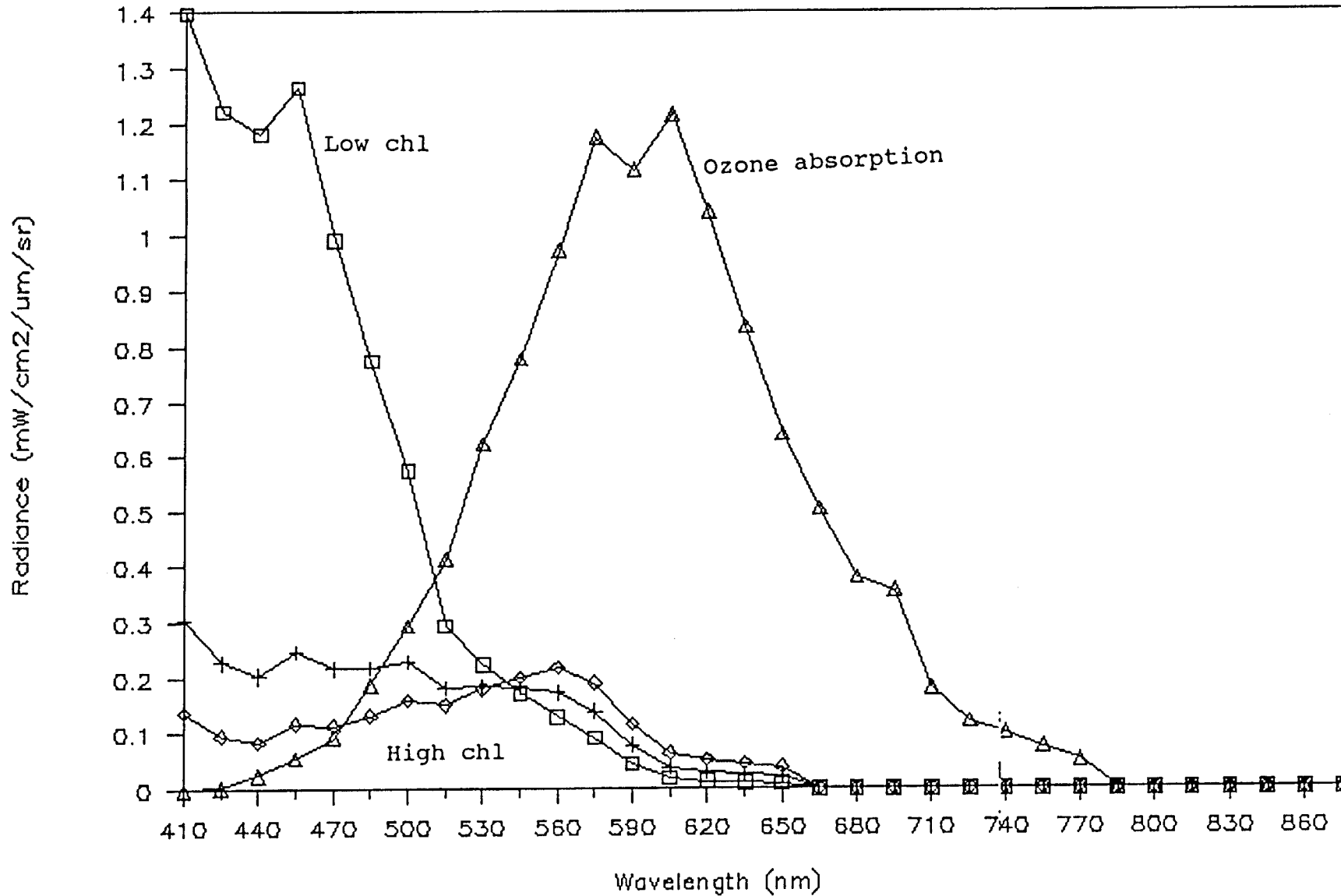


Figure 5. Normalized water-leaving radiance distribution at MODIS-T wavelengths for low ($\approx 0.05 \text{ mg m}^{-3}$), medium ($\approx 0.9 \text{ mg m}^{-3}$) and high ($\approx 8.0 \text{ mg m}^{-3}$). Also shown are ozone absorption coefficients at these wavelengths ($\times 10$).

Solar and Spacecraft Zenith Angles

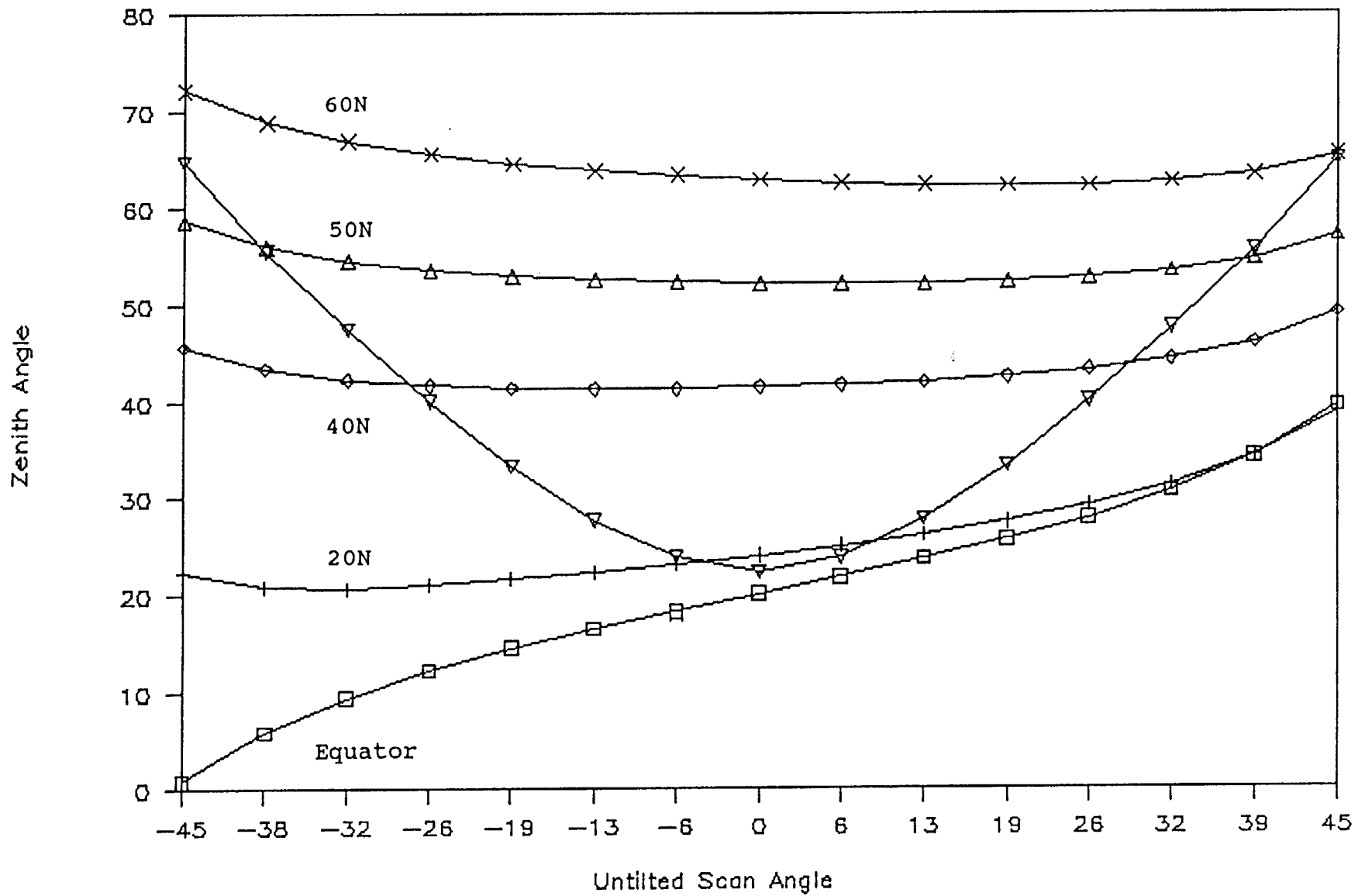


Figure 4. Distribution of solar zenith angles at Earth pixels across the satellite scan.

Radiance Error at ± 25 DU

Aerosol Radiance

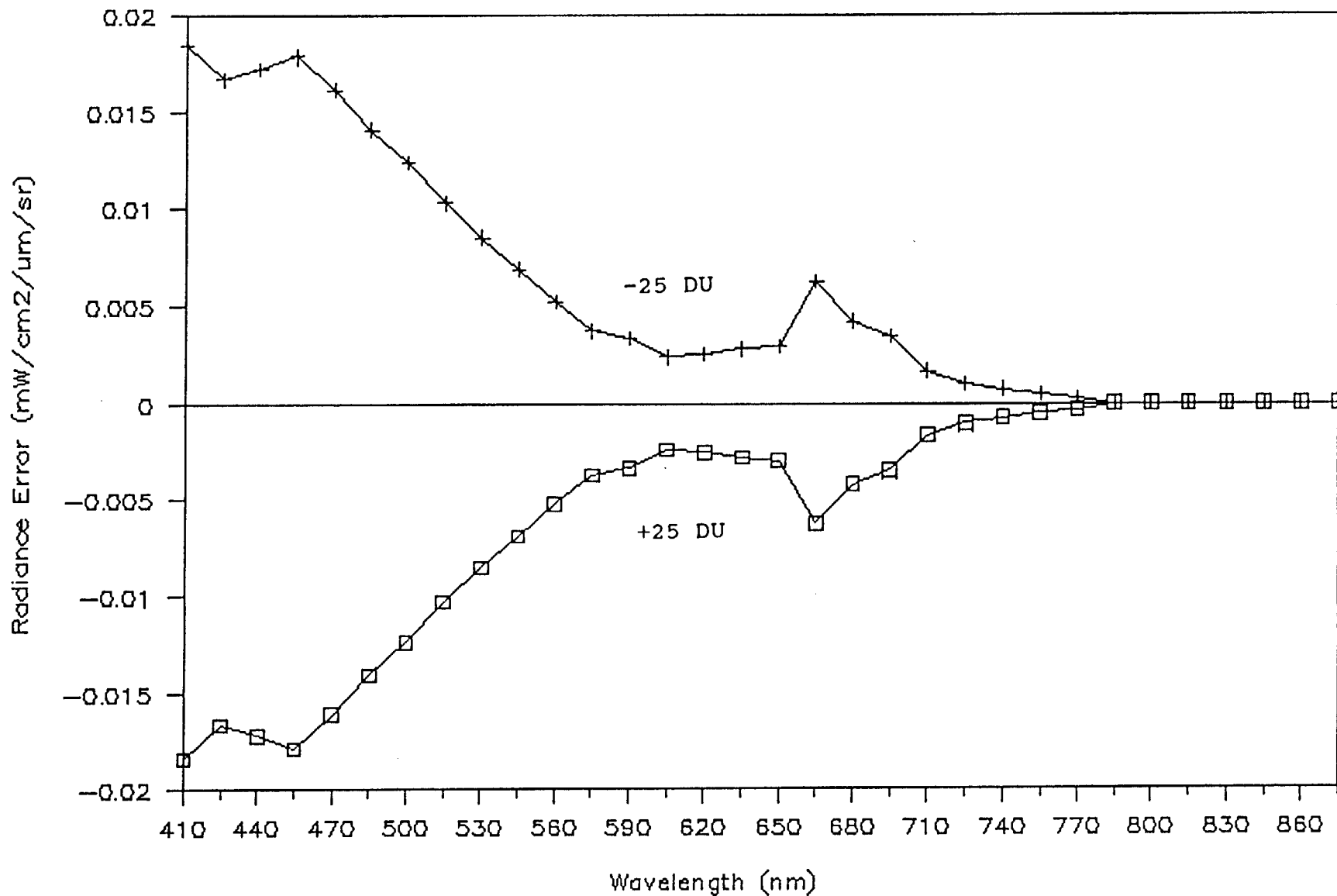


Figure 6. Error in aerosol radiance due to uncompensated ozone of ± 25 DU as computed from the atmospheric correction algorithm.

Radiance Error at ± 25 DU

Normalized Water-Leaving Radiance

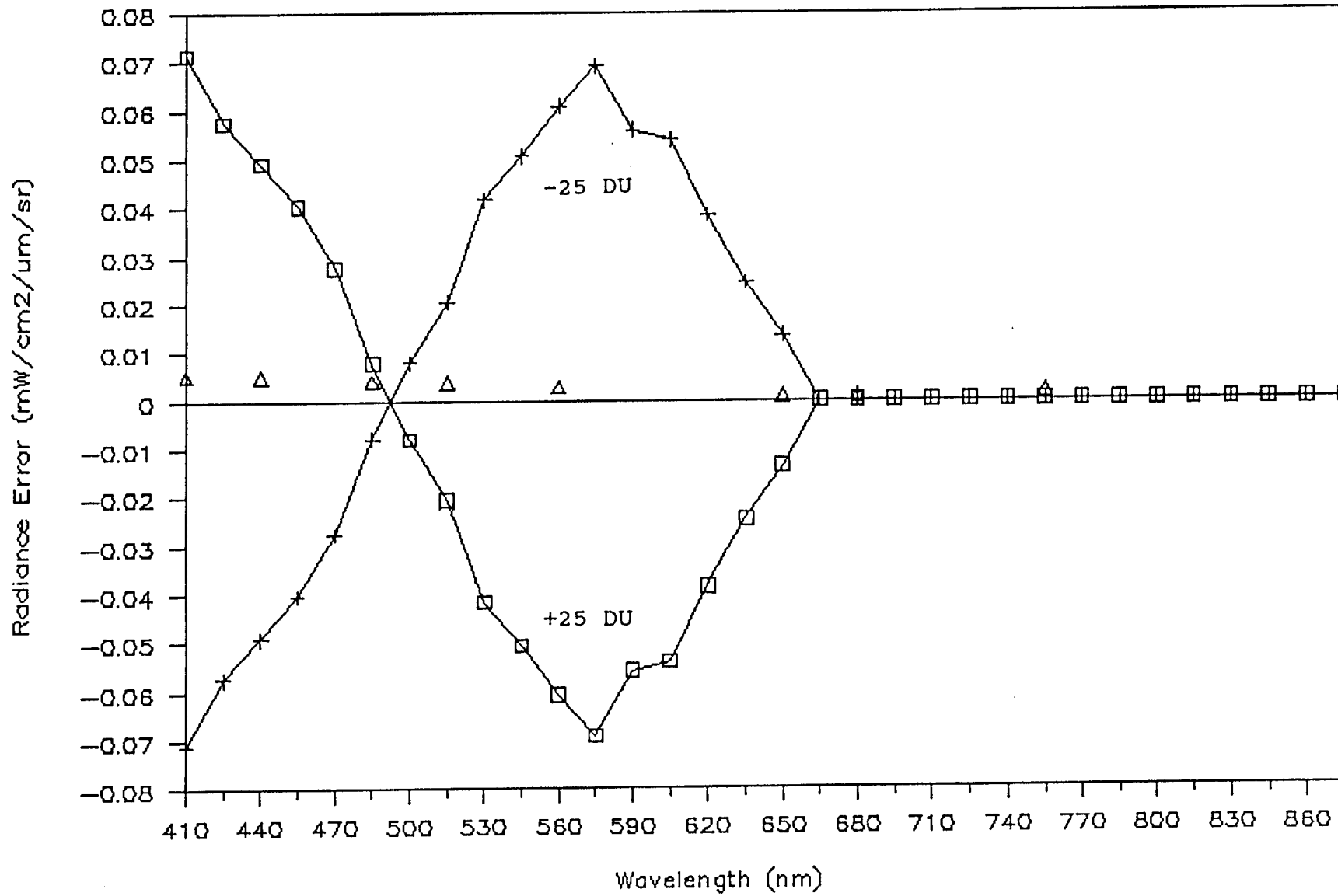


Figure 7. Error in normalized water-leaving radiance due to uncompensated ozone of ± 25 DU as computed from the atmospheric correction algorithm.

Radiance Error Lw(440)

Sub-Satellite at Equator

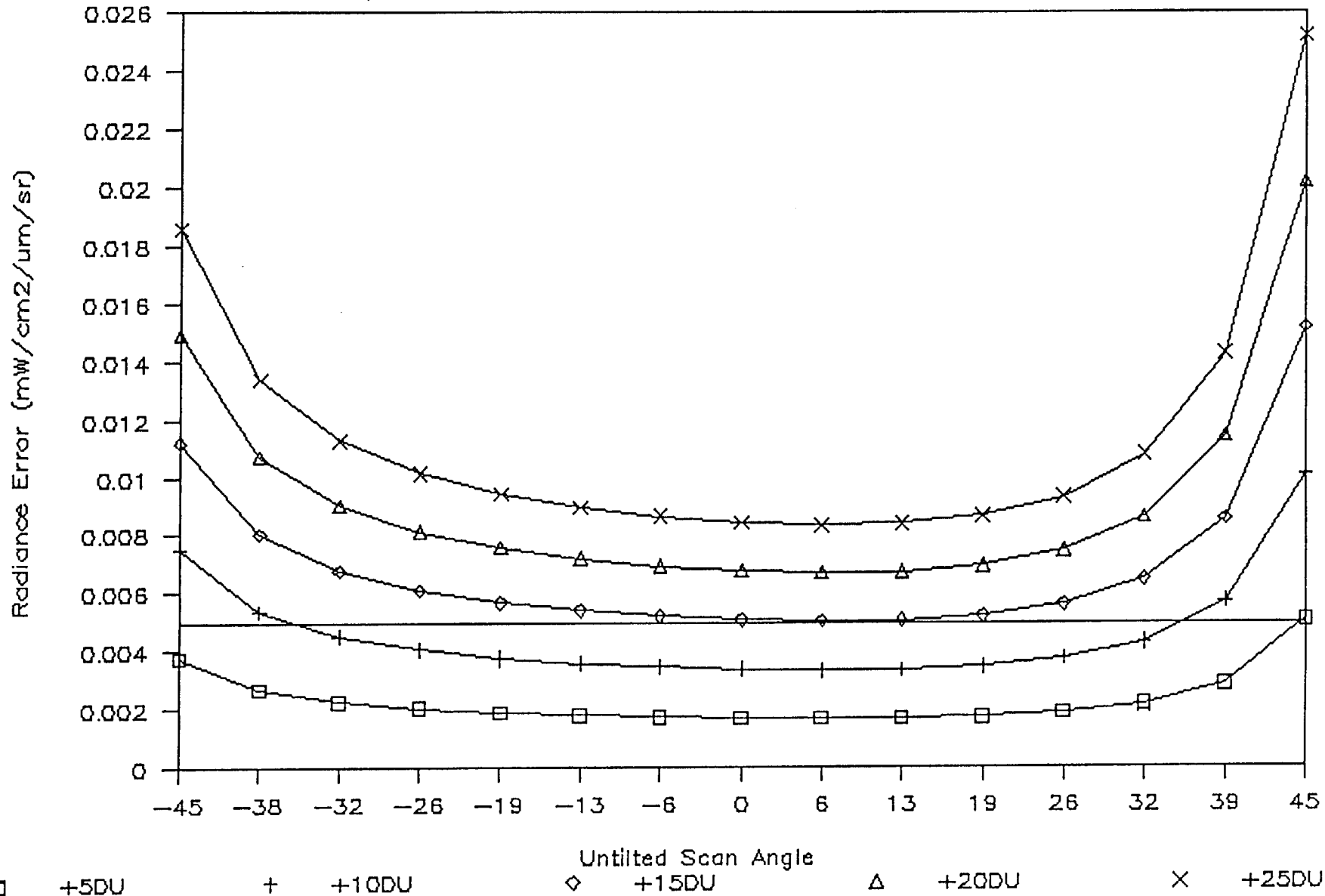


Figure 8. Error in $[L_w(440)]_N$ due to uncompensated total ozone of amounts shown for a sub-satellite point at the Equator. The abscissa depicts the untilted scan angle, but it is important to point out that these simulations were performed for a 20° tilted sensor. The unmarked straight line represents the MODIS-N NEDL.

Radiance Error Lw(560)

Sub-Satellite at Equator

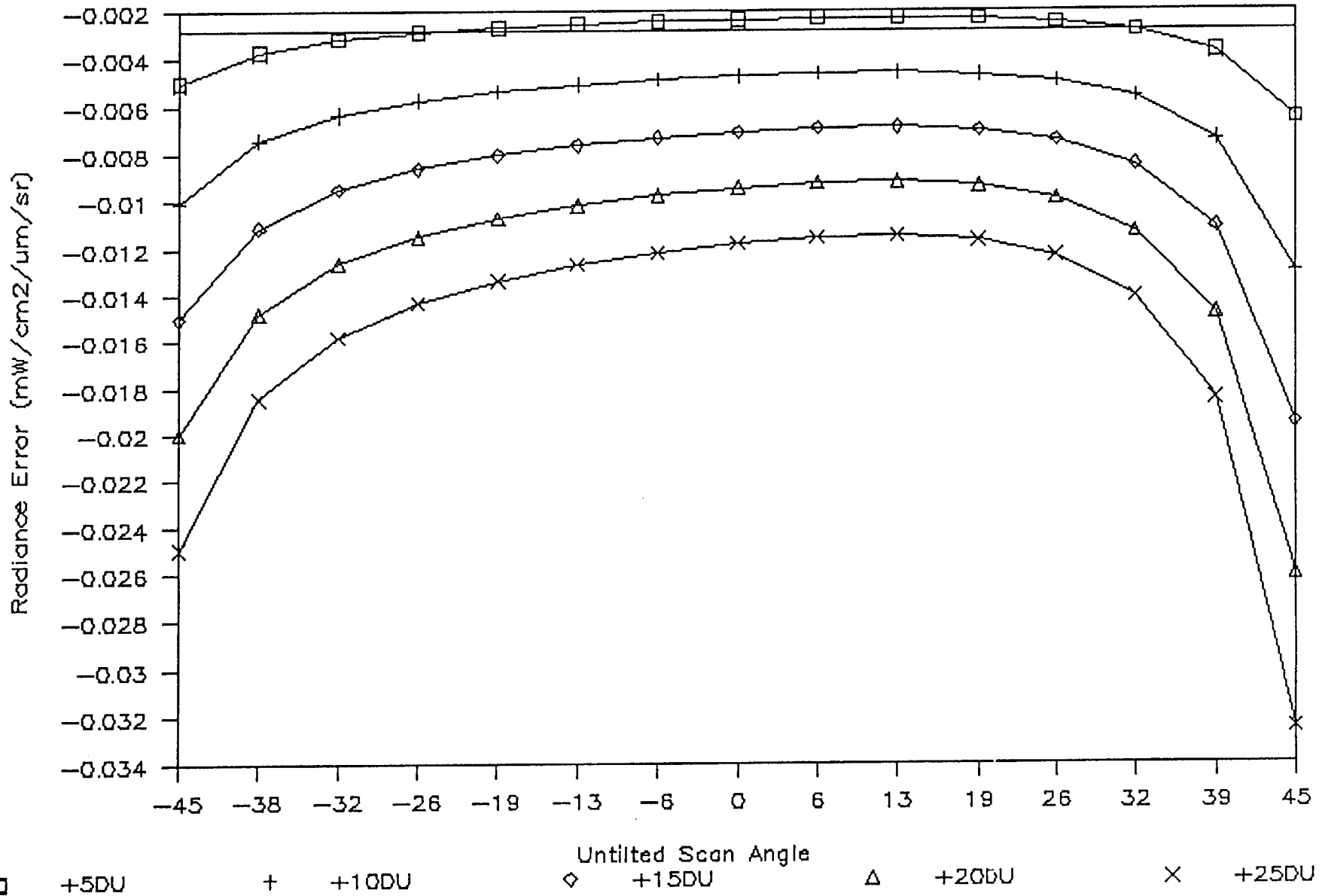


Figure 9. As in Figure 8 for $[L_w(560)]_N$.

Radiance Error Lw(440)

Sub-Satellite at 50N

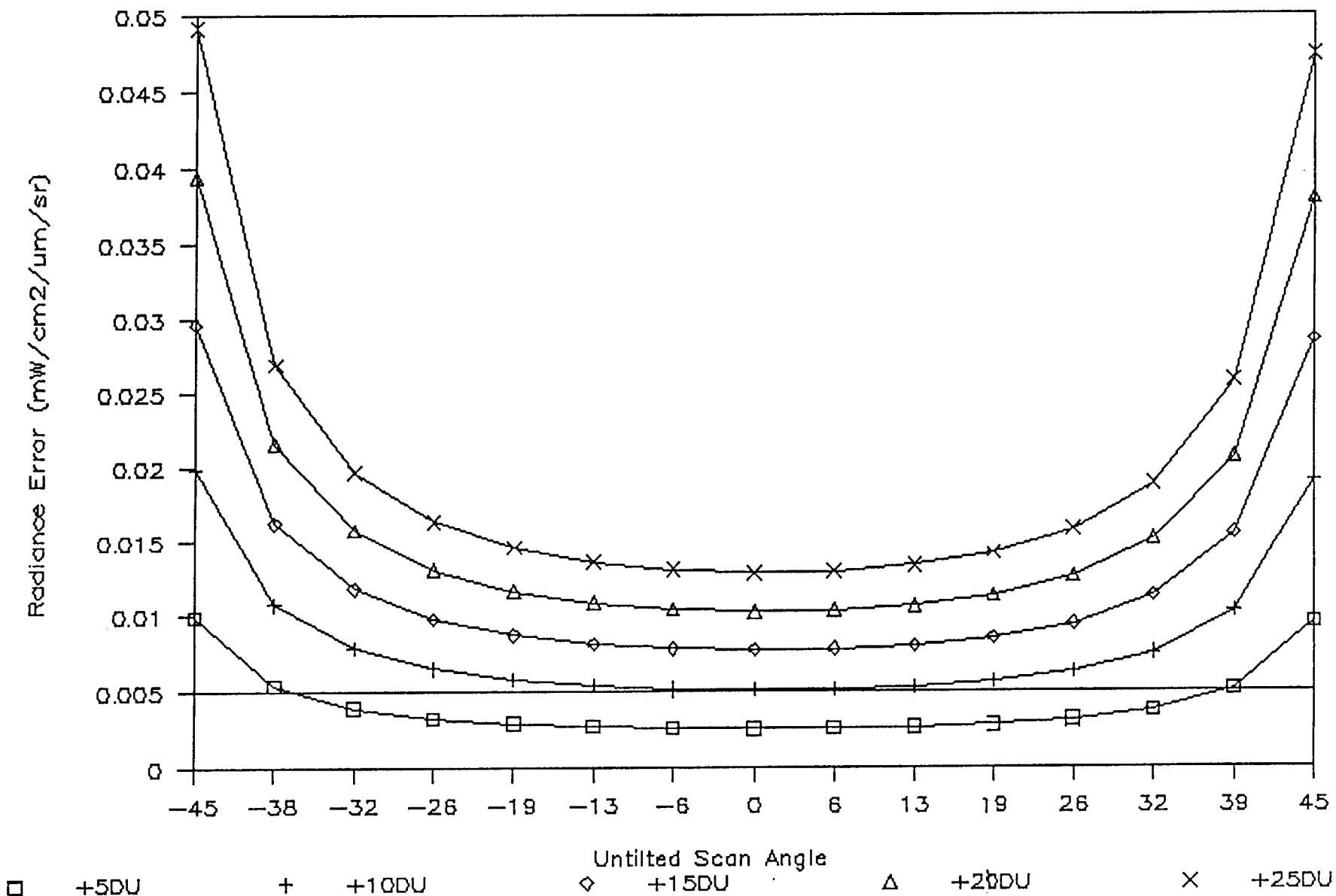


Figure 10. Error in $[L_w(440)]_N$ due to uncompensated total ozone of amounts shown for a sub-satellite point at $50^\circ N$. The unmarked straight line represents the MODIS-N NEdL.

Radiance Error Lw(560)

Sub-Satellite at 50N

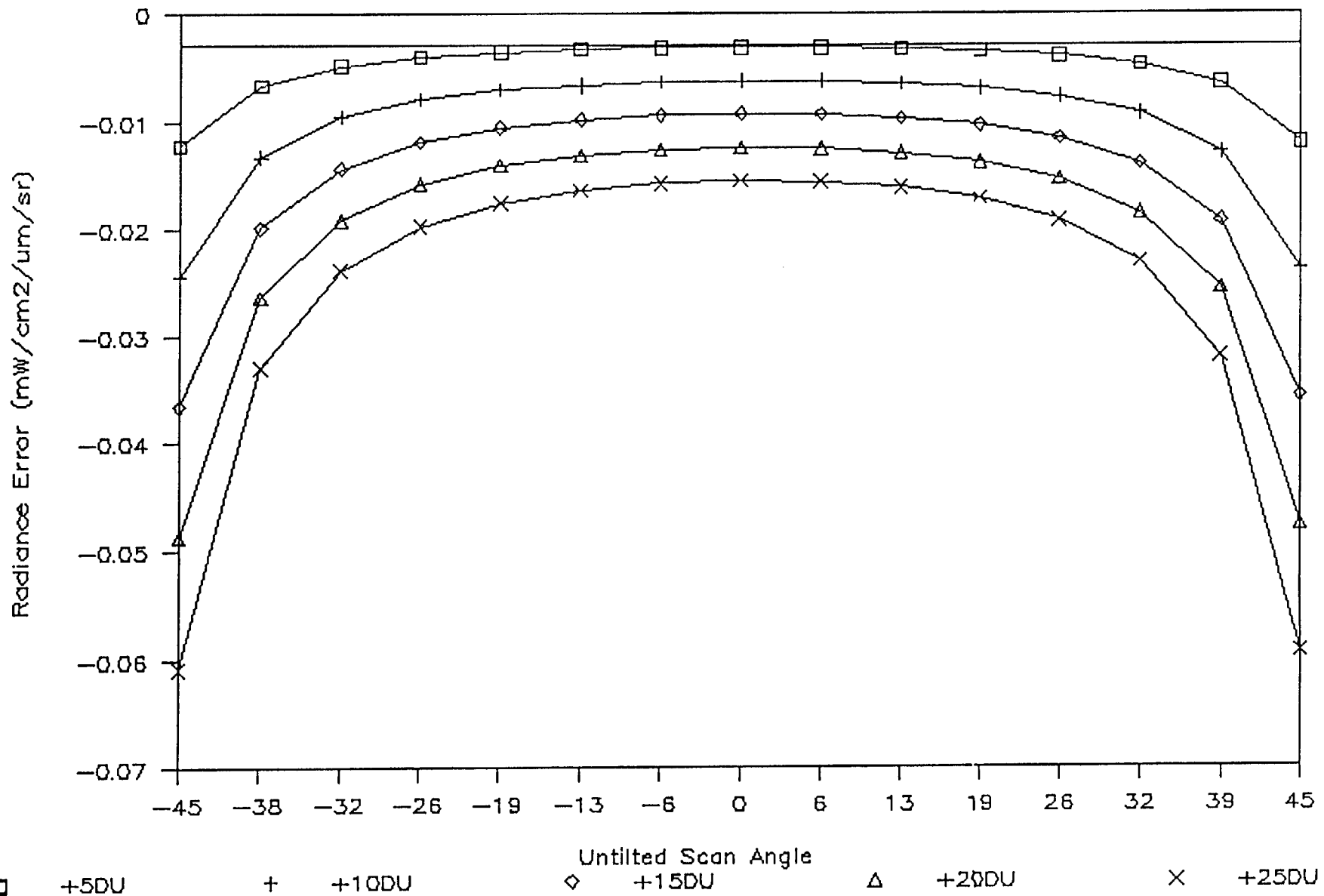


Figure 11. As in Figure 10 for $[L_w(560)]_N$.

Percent Error in Chlorophyll

Sub-Satellite at 50N

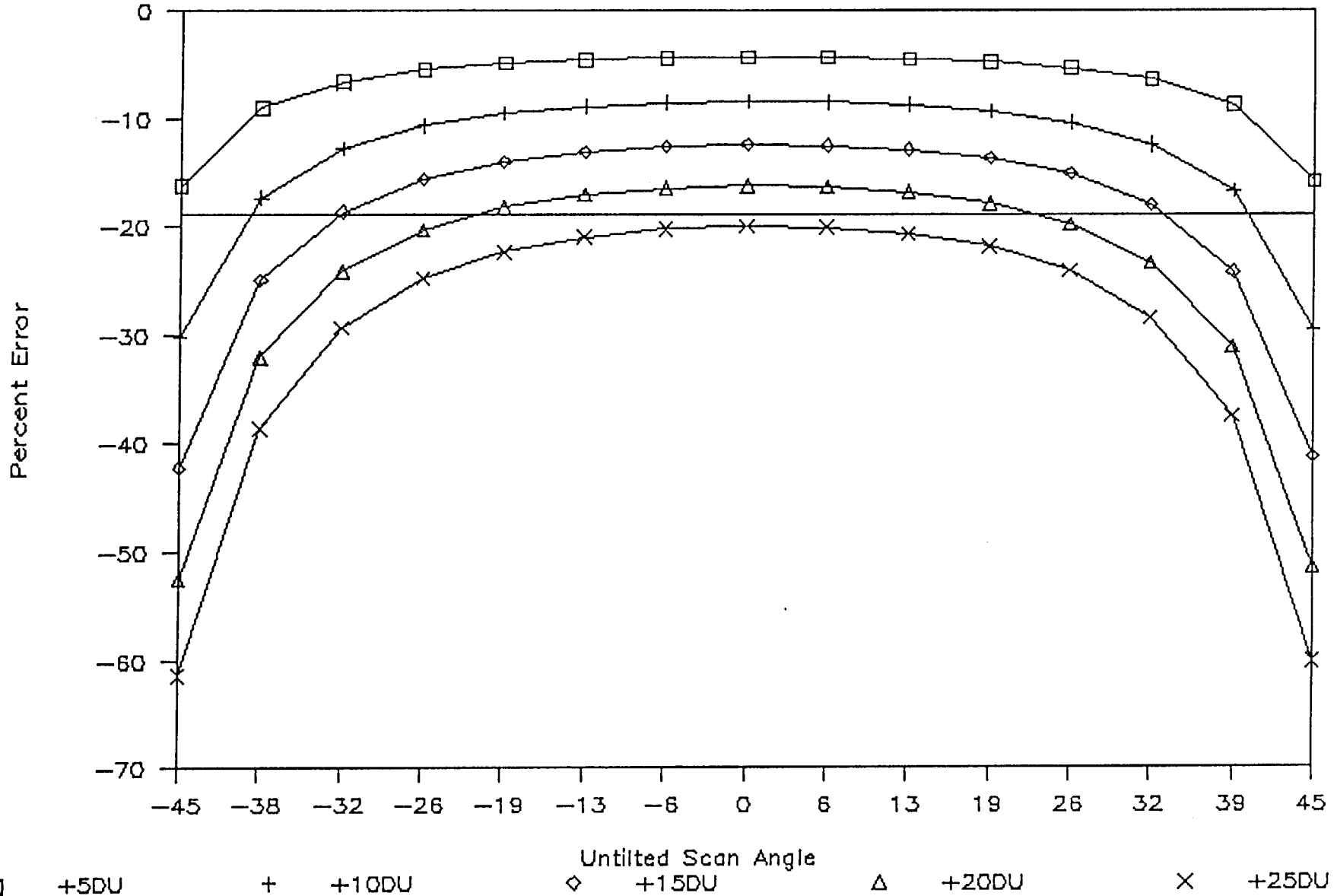


Figure 12. Percent error in chlorophyll at a sub-satellite ground point at 50°N. The straight unmarked line indicates the inherent error in the bio-optical algorithm.

Normalized Water-Leaving Radiance

Rayleigh Optical Thickness (x 3)

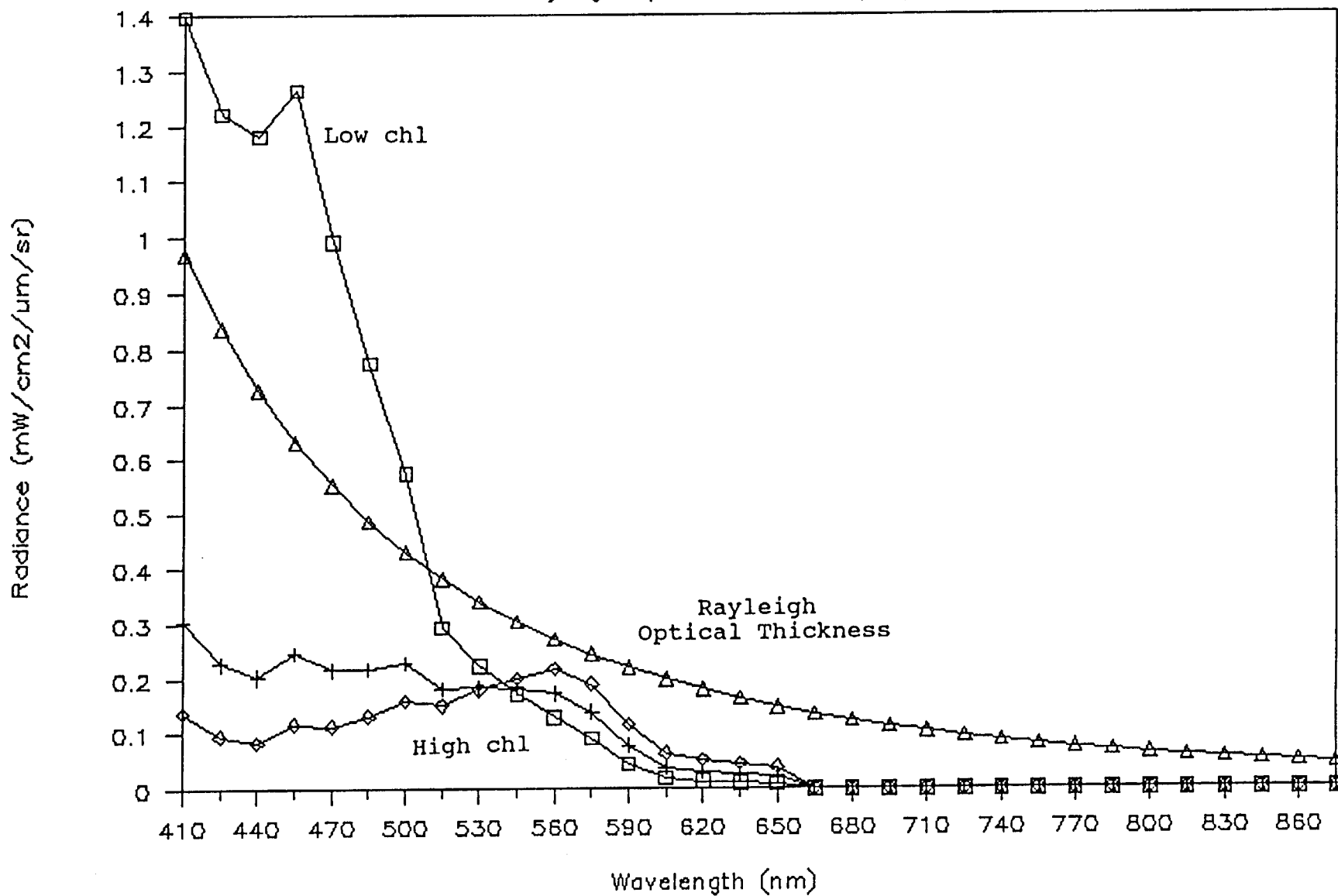


Figure 13. Normalized water-leaving radiance distribution at MODIS-T wavelengths for low ($\approx 0.05 \text{ mg m}^{-3}$), medium ($\approx 0.9 \text{ mg m}^{-3}$) and high ($\approx 8.0 \text{ mg m}^{-3}$). Also shown are Rayleigh optical thickness at standard pressure at these wavelength (x 3).

Radiance Error at ± 10 mb

Aerosol Radiance

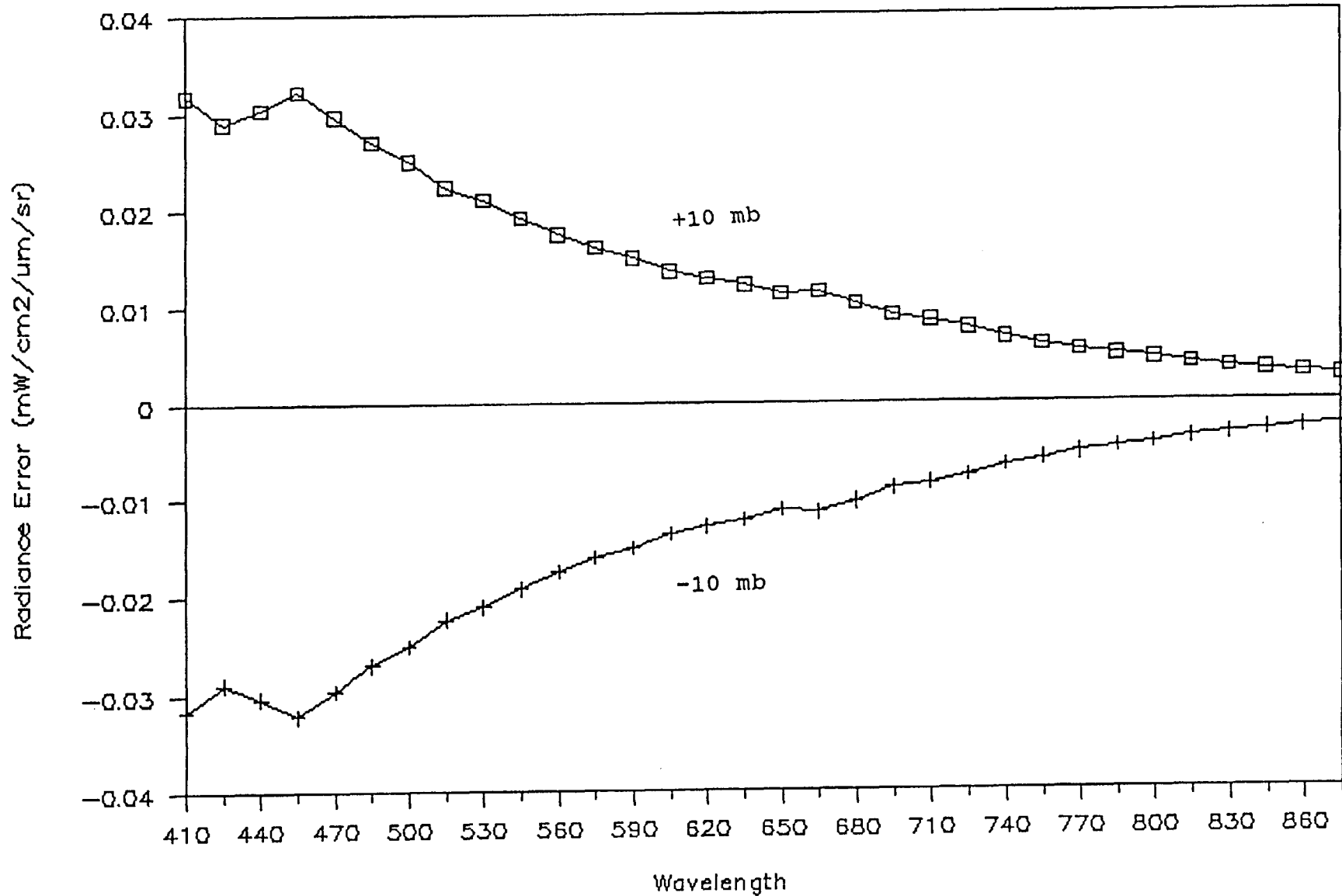


Figure 14. Error in aerosol radiance due to uncompensated atmospheric pressure of ± 10 mb as computed from the atmospheric correction algorithm.

Radiance Error at ± 10 mb

Normalized Water-leaving Radiance

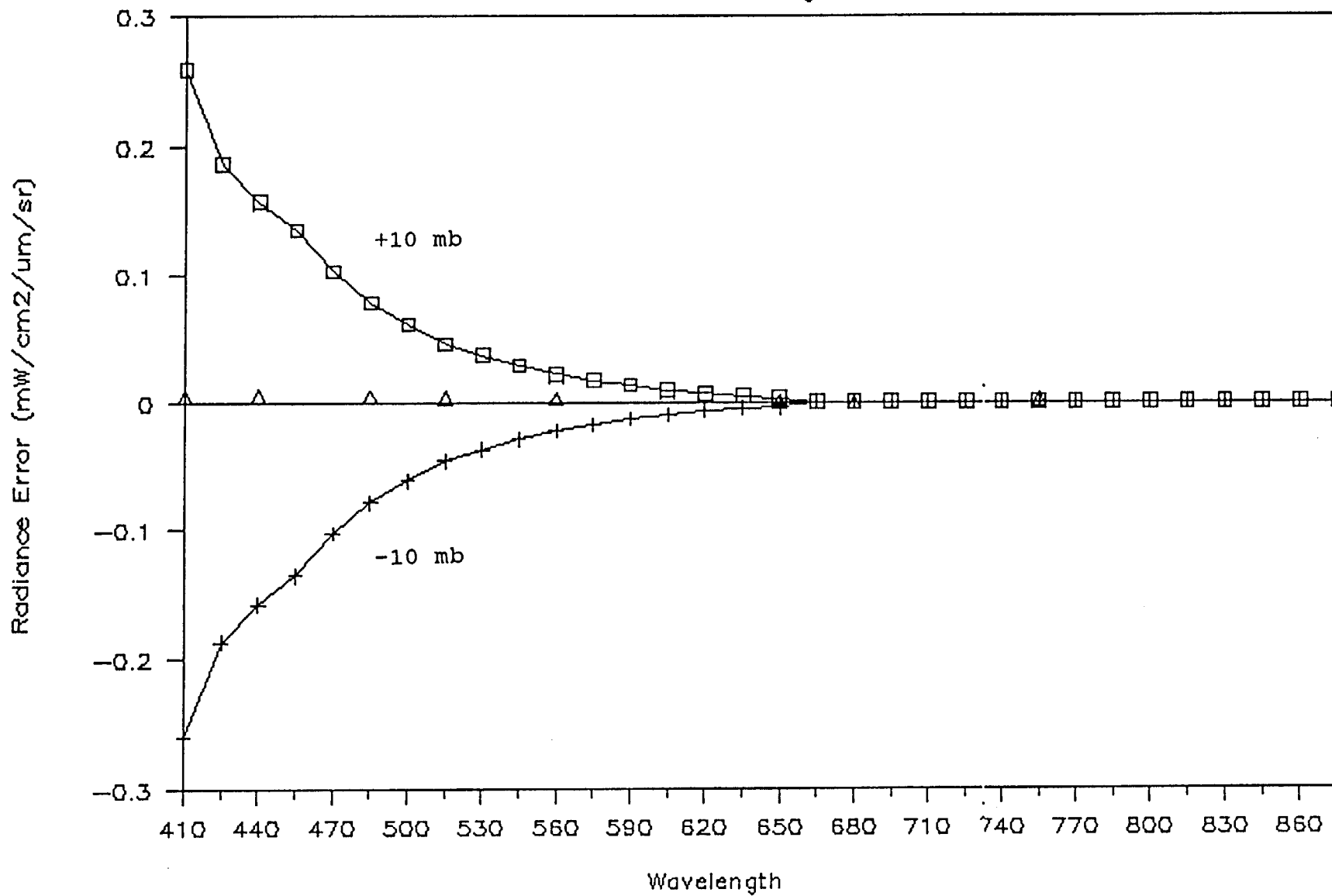


Figure 15. Error in normalized water-leaving radiance due to uncompensated atmospheric pressure of ± 10 mb as computed from the atmospheric correction algorithm.

Radiance Error Lw(410)

Sub-Satellite at 50N

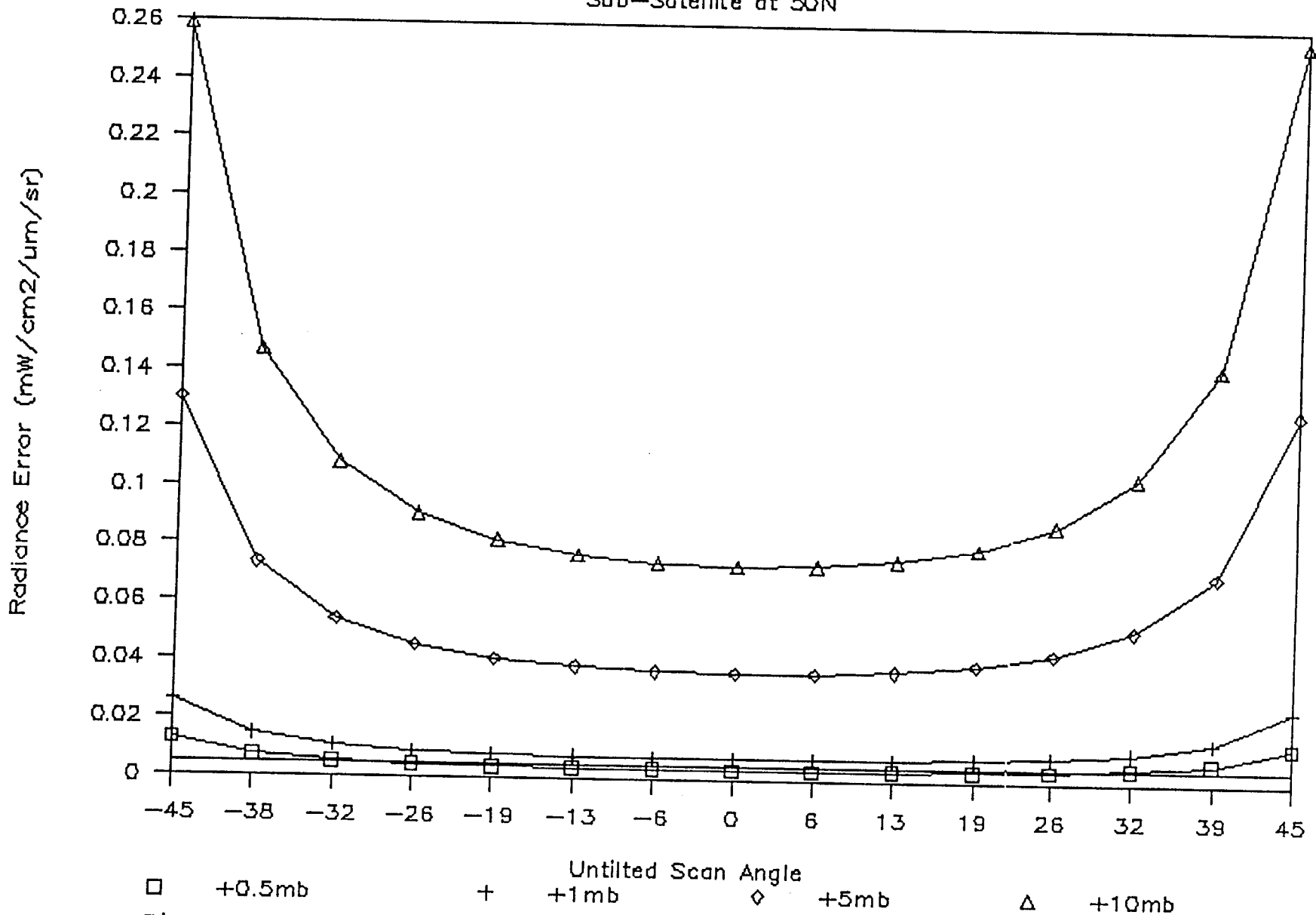


Figure 16. Error in $[L_w(410)]_N$ due to uncompensated atmospheric pressure of amounts shown for a sub-satellite point at the Equator. The abscissa depicts the untilted scan angle, but it is important to point out that these simulations were performed for a 20° tilted sensor. The unmarked straight line represents the MODIS-N NEdL.

Radiance Error Lw(440)

Sub-Satellite at 50N

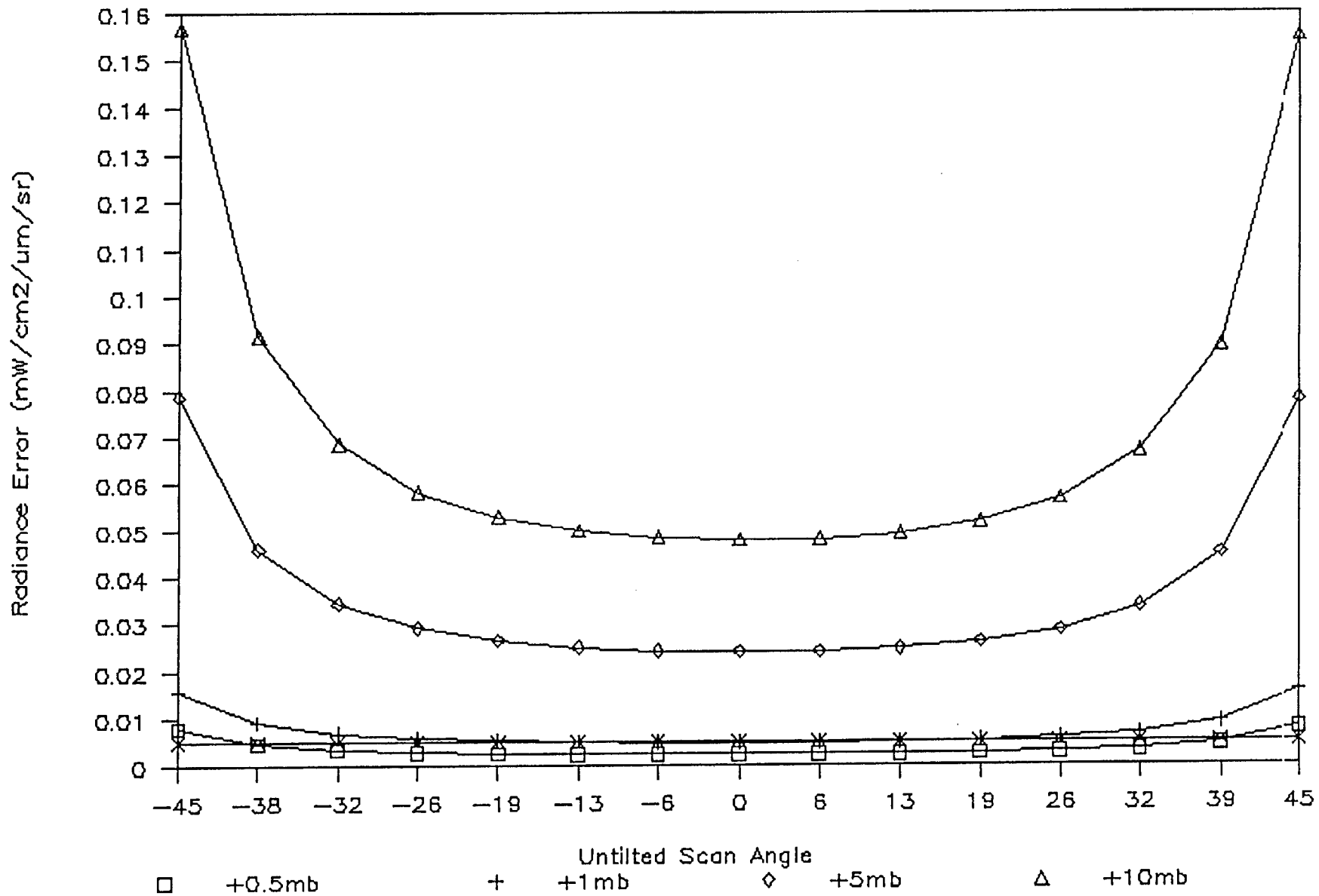


Figure 17. As in Figure 16 for $[L_w(440)]_N$.

Percent Error in Chlorophyll

Sub-Satellite at 50N

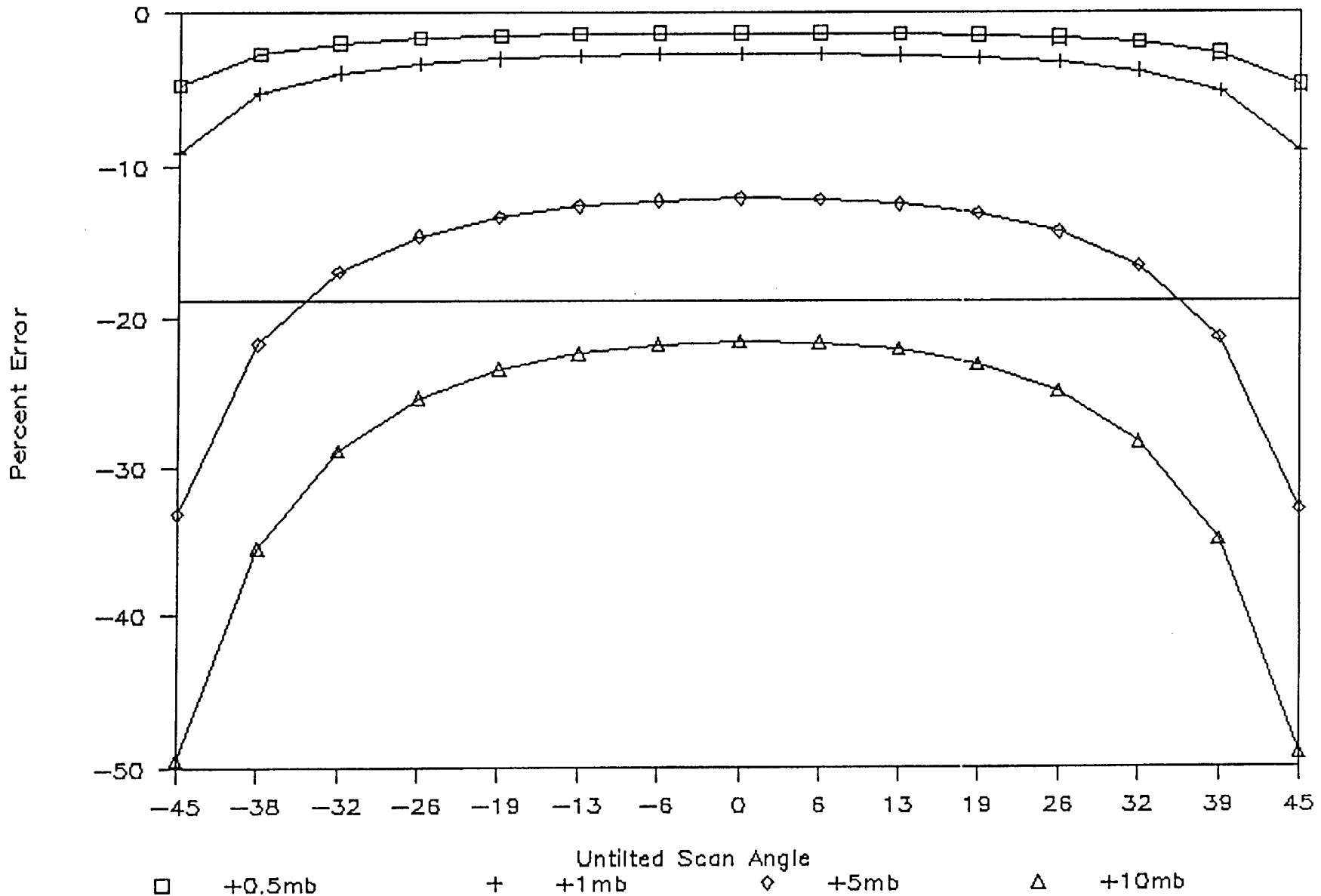


Figure 18. Percent error in chlorophyll at a sub-satellite ground point at 50°N. The straight unmarked line indicates the inherent error in the bio-optical algorithm.

3. Science Processing Support Office, SPSO

The Science Processing Support Office (SPSO) may be one of the primary interfaces between the scientists and the project. The SPSO and SDST will serve very similar functions, with the SPSO provide project wide support and the SDST providing MODIS specific support. It is anticipated that at least some of the MODIS Team Members (and the SDST) will actively interact with the SPSO. We have identified five areas in which the SPSO will provide support on a project wide basis.

First, the SPSO will be responsible for information management. The SPSO will collect any available information from Team Members and any other appropriate source. This information will be collected in a database and be made available to the project, Team Members, and the potential user community. This activity is already in progress.

Second, the SPSO should establish a pre-launch data archive which will contain data of general use to the entire Team Member community. This archive is clearly required to accomplish the Eos mission. In particular, data will be needed for algorithm development and testing. It is appropriate that this data be collected and distributed by the project.

Third, the SPSO will provide project wide coordination and communication. This will include activities like requirements reviews and identifying instrument inter-dependencies.

Fourth, the SPSO will develop software utilities of general use to scientists across the project. This might include standard I/O routines and coordinate transformations. The SPSO will develop software for the Information Center (IMC) and to display browse data.

Finally, the SPSO will support CDHF software integration and reprocessing. This will be done, in part, at a project wide level. It is anticipated that each science team will produce fully integrated software and that the SPSO will integrate the integrated packages of the various team. The SPSO will also oversee the reprocessing from a system wide prospective.

4. MODIS Science Team Members

The MODIS Science Team Members will be responsible for accomplishing the scientific objectives of their personal research, that of the MODIS science team, and that of the Eos project. The Science Team will fully define their role within the requirements established by the project. The Science Team will also determine the support needed from the SDST. It is anticipated that the Team Members and the SDST will work closely together.

The primary function of the Science Team Members will be to establish a set of science products and to develop the algorithms needed to generate those products. The Team Members will validate the data products produced by those algorithms.

The Science Team Members will be responsible for obtaining the correlative data needed for their products. (Some of this data may be collected on a project wide basis. However, if certain correlative data are required, the Team Members is ultimately responsible.) The data collection and validation activities will include planning and conducting field campaigns.

The Team Members will conduct scientific analyses of data and data products. An important part of this activity will be the reporting of the scientific results and data sets both in peer reviewed scientific literature and meetings.

5. MODIS Science Data Support Team

The general mission of the Science Data Support Team (SDST) will to support the Team Members. The functions of the SDST will be defined by the MODIS Science Team. In practice, the SDST will be required to do "everything" that is not done someplace else. At this time, we have developed a preliminary list of fifteen functions for the SDST. Many of these functions are similar to those expected of the SPSO. The difference is that the SDST will primarily address MODIS specific issues. The SDST should be viewed as "working for" and performing support functions for the Team Members

The SDST, as it evolves from the MODIS data study team, will continue to collect

and update requirements from the Science Team. The requirements of the individual scientists will be integrated to establish a single set of requirements for MODIS. These requirements will be given to the Eos project. The SDST will continue to review the development of EosDIS, CDOS, the platform, and other institutional elements to determine that the MODIS specific requirements are met. Many of these functions will be shared with the SPSO and/or the Team Members.

The SDST may assist with the coordination of algorithm development. This might be required to avoid unintended duplication of effort and to ensure that all of the required algorithms are developed, particularly the utility and support algorithms. The SDST will aid the Team Members in algorithm development. While the Team Members will be required to deliver fully developed working algorithms, it is anticipated that the SDST could provide support in prototyping, debugging, testing, and integrating the algorithms.

The SDST will optimize algorithms for use on the CDHF computers. If required, this may involve the SDST working with the science Team Member to modify the code developed by the Team Members. As part of this process, data dependencies will be identified. It will be necessary to ensure that all of the data required for each algorithm is available at the CDHF with the required timeliness. It is possible that the SDST will play a role in meeting the requests for MODIS data from other Eos investigators or teams. The SDST will integrate the individual algorithms into a global MODIS processing package. The SDST will ensure that the total package functions as required.

It would be appropriate to have the SDST help with the documentation of the algorithms. This would ensure that the project's documentation standards were met and uniform documentation for all MODIS algorithms produced. The SDST could also assist with the provision of the required user's guides and manuals. The SDST will maintain the algorithms and make any modifications necessary as hardware changes are made at the CDHF. (It is not anticipated that the SDST will maintain specialized algorithms at the Team Member facilities.)

The SDST will actually develop some algorithms. It is anticipated that the SDST will write the Level-1 processing software. The SDST will also develop standard utilities which can be used by any and all MODIS Science Team Members.

The Science Team Members will be responsible for validating the MODIS science products. The SDST may assist in this effort. After validation, the science products will continue to be reviewed on a daily basis. This will probably be done by the SDST with the Team Members being involved only occasionally or as problems are detected.

The SDST can help to coordinate the data collection activities of the Team Members. This will include the collection of correlative data and perhaps field experiment support. The SDST may assist Team Members to reformat data collected by Team Members to meet project standards and allow it to be archived in the DADS. The SDST can also help to ensure that project standards are met on specialized products and algorithms that are ultimately included in the archive.

The SDST can help to coordinate and manage Near-Real-Time processing which will typically be done to support field experiments. In particular, Near-Real-Time processing may require operator intervention, which would be done either by the Team Member or the SDST. Finally, the SDST can help to coordinate and manage the reprocessing of MODIS data. Reprocessing may involve modifications to the standard software package. The SDST could help with these modifications and otherwise ensure that the required reprocessing is successfully completed.

The following table summarizes the functions discussed above.

Table 1. Candidate Functions of the EosDIS/Eos Project, the EosDIS Science Processing Support Office, the MODIS Science Team Members, and the Science Data Support Team.

| |
|---|
| EosDIS/Eos PROJECT |
| <ul style="list-style-type: none"> • Provide Hardware • Establish Standards • Levy Requirements |
| SCIENCE PROCESSING SUPPORT OFFICE |
| <ul style="list-style-type: none"> • Information Management • Establish Pre-Launch Data Archive • Coordination Across the Project • Develop Project Utilities • Integrate Software |
| MODIS SCIENCE TEAM MEMBERS |
| <ul style="list-style-type: none"> • Develop Science Products and Algorithms • Validate Products • Collect Data Conduct Field Campaigns • Analyze Data and Science Products • Report Results |
| SCIENCE DATA SUPPORT TEAM |
| <ul style="list-style-type: none"> • Collect/Develop/Review Requirements • Develop and Follow Prototyping Plan • Provide Simulated MODIS Data • Coordinate Algorithm Development • Aid in Debugging and Testing Algorithms • Optimize Algorithms for the CDHF • Identify Data Dependencies • Eliminate Inconsistencies in Common Tasks • Integrate MODIS Algorithms (Levels 1-4) • Document Algorithms • Develop User's Manuals • Maintain Algorithms • Write Level-1 Software • Write MODIS Software Utilities • Coordinate Data Collection • Maintain Eos Standards for Specialized Products • Coordinate/Manage Near-Real-Time Processing • Coordinate/Manage Reprocessing • Other Functions Not Done Elsewhere |

SCIENCE DATA SUPPORT TEAM ROLE AND FUNCTIONS

1. Introduction

The Science Data Support Team (SDST) has been defined as part of the MODIS Team Leader Computer Facility (TLCF) with the broadly stated mission of providing support to the MODIS Science Team. In this discussion, a role for the SDST is defined. The functions of EosDIS, the EosDIS Science Processing Support Office (SPSO), and the Team Members are presented.¹ The SDST will interact closely with both the SPSO and the Team Members to execute those tasks not done by either of the above groups. Certain of the SDST's tasks will be shared with either the SPSO or the Team Members.

The SDST will consist of computer programmers, systems analysts, and science team member support personnel, all under the direction of the MODIS Science Team Leader. The SDST will require access to the Central Data Handling Facilities (CDHFs) within the EosDIS Active Archives, access to the TLCF, and communications access to the various MODIS Team Member Computing Facilities (TMCFs). It must be emphasized that the role of the SDST is conceived to assist the MODIS Team Members. Hence, the exact role of the SDST is to be defined by the Team Members (within Eos Project guidelines).

2. EosDIS/Eos Project

EosDIS and the Eos project will provide computer and communications hardware for both centralized and distributed Project and Team Member facilities. EosDIS will establish standards, which will include such categories as operating systems, programming languages, documentation, data formats, and map projections. Eos and EosDIS will levy requirements on the Team Members. The requirements will cover such things as delivery dates for software.

¹Some of the concepts presented by Al Fleig at the EosDIS All-Hands Meeting and Yun-Chi Lu at a Code 600 EosDIS meeting (September 28, 1988) have been included in this summary.